2014•2015

FACULTEIT GENEESKUNDE EN LEVENSWETENSCHAPPEN

master in de biomedische wetenschappen

Masterproef

Regulation of mitophagy by Sab during adipogenesis

Promotor :
dr. Willem VONCKEN

Promotor :
Prof.dr. JEREMY W. CHAMBERS

Copromotor :
dr. ANDREA ROMANO

Désirée Goubert

Scriptie ingediend tot het behalen van de graad van master in de biomedische wetenschappen

De transnationale Universiteit Limburg is een uniek samenwerkingsverband van twee universiteiten in twee landen: de Universiteit Hasselt en Maastricht University.

universiteit hasselt
KNOWLEDGE IN ACTION

Universiteit Hasselt | Campus Hasselt | Martelarenlaan 42 | BE-3500 Hasselt
Universiteit Hasselt | Campus Diepenbeek | Agoralaan Gebouw D | BE-3590 Diepenbeek

universiteit hasselt | Maastricht University

2014•2015
FACULTEIT GENEESKUNDE EN LEVENSWETENSCHAPPEN
master in de biomedische wetenschappen

Masterproef

Regulation of mitophagy by Sab during adipogenesis

Promotor :
dr. Willem VONCKEN

Promotor :
Prof.dr. JEREMY W. CHAMBERS

Copromotor :
dr. ANDREA ROMANO

Désirée Goubert

Scriptie ingediend tot het behalen van de graad van master in de biomedische wetenschappen

universiteit hasselt | Maastricht University

Table of Contents

Acknowledgements

I would like to express my very great appreciation to Dr. Jeremy Chambers, my primary research supervisor from the Department of Cellular Biology and Pharmacology at Florida International University, who not only accepted me in his lab as an international student but also provided me with his valuable and constructive suggestions during the planning and development of this research work. He helped me through thick and thin with administration, professional and personal development, critical thinking and writing. His willingness to give his time so generously has been very much appreciated.

I am grateful to Prof. Dr. Willem Voncken, my institutional supervisor from the Department of Molecular Epigenetics at Maastricht University, for his permanent encouragement and patient guidance to do an international internship. I am also thankful for the help he provided me in writing the proposal that preceded the senior practical training and for the open communication we had during the internship.

I would like to extend my thanks to all my colleagues with whom I worked closely together in the Chamber's lab and who provided me help and practical advice when needed. I appreciate the research support from Sarah Igbal and Graham West, from the Scripps Research Institute Florida.

Also, I am extremely blessed with all of my friends who were there to talk to and support me. The international network I build up during my experience helped me to develop an open mindset and an international network to fall back on during the development of my future career.

Finally, I would like to take this opportunity to express my gratitude towards my parents and grandparents, who raised me as the motivated and passionate woman I am today and who stood by my side during all the years of my studies. Special "thanks" to Alexander Gerben who was always there for moral support and who stood by my side throughout my entire education.

Altogether, I am extremely happy to have had the opportunity to do my senior internship in USA, for which I should also thank Miss Liesbeth Oeyen who helped me with the administration and financial aspects. Being in my final year as a master student, this experience prepared me extremely well to start a blossoming career in science.

Abbreviations

Acetyl Co-A	Acetyl coenzyme A	**PBS**	Phosphate-buffered saline
WHO	World health organization	**HBSS**	Hank's balanced salt solution
BMI	Body mass index	**BCA**	Bicinchoninic acid
DALYs	Disability adjusted life years	**CV**	Coefficient of variance
C/EBP	CCAAT/enhancer-binding protein	**SDS-PAGE**	Sodium dodecyl sulfate polyacrylamide gel electrophoresis
PPAR-γ	Peroxisome proliferator activated receptor-γ	**PVDF**	Polyvinylidene fluoride
ATP	Adenosine triphosphate	**TBS**	Tris-buffered saline
FA	Fatty acid	**BSA**	Bovine serum albumin
Atg	Autophagy gene	**RT**	Room temperature
JNK	c-Jun N-terminal kinase	**AMPKα**	5' adenosine monophosphate-activated protein kinase α
MAPK	Mitogen-activated protein kinase	**SIRT**	Sirtuin
SAPK	Stress-activated protein kinase	**mTOR**	Mammalian target of rapamycin
MAPKK	MAPK kinases	**COX-IV**	Cytochrome c oxidase, or complex IV
MAPKKK	MAPKK kinases	**mtTFA**	Mitochondrial transcription factor A
AP1	Activator protein-1	**LB**	Lauria Broth
ROS	Reactive oxygen species	**siRNAs**	Small interfering ribonucleic acids
T2D	Type 2 diabetes	**FABP4**	Fatty acid binding protein 4
ASK1	Apoptosis signaling regulated kinase 1	**ERK**	Extracellular-signal-regulated kinase
OMM	Outer mitochondrial membrane	**ORF**	Open reading frame
Bcl-2	B-cell lymphoma 2	**RFP**	Red fluorescent protein
shRNA	Small hairpin RNA	**KIM1**	Kinase interaction motif 1
DMEM	Dulbecco's Modified Eagle Medium	**Mfn2**	Mitofusin 2
FBS	Fetal bovine serum	**UCP1**	Uncoupling protein 1
DEX	Dexamethasone	**IBMX**	Iso-butylmethylxanthine
NCS	Newborn calf serum		
BM I	Basal medium I		
DM I	Differentiation medium I		
BM II	Basal medium II		
DM II	Differentiation medium II		

Summary

Introduction: Obesity is a global epidemic. Adipogenesis, the synthesis of fat, is elevated in obese individuals. During adipogenesis, mitochondrial density is reduced by a form of self-digestion called mitophagy. Mitophagy is essential to adipogenesis; however, the molecular mechanisms regulating mitophagy are unknown. Existing data suggests that signaling complexes on the outer mitochondrial membrane, such as Sab, facilitate mitophagy. In the present project, the role of post-translational modifications on Sab, in mitochondrial turnover during adipogenesis was investigated. Based on preliminary results we hypothesize that **acetylation of Sab on lysine 6 (K6) promotes mitophagy during adipogenesis.**

Materials and methods: To explore this hypothesis in a model of adipogenesis, 3T3-L1 mouse pre-adipocytes were differentiated into adipocytes. Cells were lysed at distinct times and subjected to western blot analysis, or mass spectrometry analyses to evaluate Sab abundance and post-translational modifications. Further, the effect of differentiation agents and metabolic context on Sab expression was evaluated in a similar manner. Finally, gene silencing was employed to determine the impact of sirtuins on Sab concentration and stability.

Results: Sab expression increased during adipogenesis and preceded mitophagy. Protein analysis revealed that Sab is acetylated during adipogenesis. Individual differentiation agents did not affect Sab expression or acetylation; however, palmitate increased both Sab and acetyl-Sab levels. Silencing sirtuins revealed that Sirtuin 3, a mitochondrial isoform, increased acetylated Sab. Sab:K6A and Sab:K6E mutants did not localize to mitochondria and formed aggregates.

Discussion and conclusion: Sab expression increased in response to elevated levels of fatty acids during adipogenesis. As a result of nutrient excess, Acetyl Co-A levels increased in mitochondria leading to Sab acetylation and stabilization. Sab-mediated signaling in turn targets mitochondria for degradation. Also, lysine 6 of Sab is necessary for the mitochondrial localization of Sab. The results demonstrate that Sab is required for adipogenesis and represent a novel target for anti-obesity therapeutics.

Samenvatting

Introductie: Obesitas is een wereldwijde epidemie. Obese patiënten hebben kenmerkend een toegenomen adipogenese, het syntheseproces van vetten. Gedurende de adipogenese daalt de dichtheid van mitochondriën door mitofagie, de zelf-vertering van mitochondriën. Hoewel de onderliggende mechanismen niet bekend zijn, is mitofagie van essentieel belang voor de adipogenese. Bestaande gegevens geven aan dat signaalcomplexen op de buitenste mitochondriale membraan, zoals het eiwit Sab, mitofagie faciliëren. Gedurende het huidige project werd de rol van post-translationele modificaties in Sab in de context van mitochondriale veranderingen tijdens adipogenese onderzocht. Aan de hand prelimaire studies veronderstelde ons team dat **acetylering van Sab op lysine 6 (K6) mitofagie bevordert gedurende de adipogenese.**

Materiaal en methoden: Om onze hypothese te onderzoeken in een adipogenesemodel, werden 3T3-L1 muis pre-adipocyten gedifferentieerd tot adipocyten. Cellen werden op verschillende tijdstippen gelyseerd en onderworpen aan western blot, of massaspectrometrieanalyses ter evaluatie van de hoeveelheid Sab en post-translationele modificaties. Tevens werd het effect van individuele differentiatiecomponenten en metabole context op Sab expressie op een gelijkaardige manier geëvalueerd. Tot slot werd gene silencing uitgevoerd om de impact van sirtuïnes op de Sab-concentratie en -stabiliteit te bepalen.

Resultaten: Adipogenese vertoonde een gestegen Sab-expressie welke mitofagie voorafgaat. Eiwit analyse toonde aan dat Sab geacetyleerd is tijdens adipogenese. Individuele differentiatiecomponenten beïnvloedden de Sab-expressie of -acetylering niet. Palmitaat daarentegen verhoogde de al dan niet geacetyleerde Sab-niveaus. Bijkomend leidde Sirtuïne 3 silencing tot toename in de hoeveelheid geacetyleerde Sab-eiwitten. De Sab:K6A en Sab:K6E mutanten vormden aggregaten, welke niet naar de mitochondriën lokaliseerden.

Discussie en conclusie: Verhoogde vetzuurniveaus induceerden Sab-expressie gedurende adipogenese. Een overvloed aan nutriënten veroorzaakt een toename in mitochondriaal Acetyl Co-A, wat leidde tot acetylering en stabilisatie van Sab. De Sab-gemedieerde signalisatie beïnvloedt op zijn beurt de mitochondriale degradatie. Tevens is lysine 6 noodzakelijk voor de mitochondriale lokalisatie van Sab. De resultaten tonen de noodzakelijkheid van Sab aan gedurende adipogenese en stellen een nieuw doelwit voor anti-obesitas therapieën voor.

Chapter 1
Introduction

1.1 Adipogenesis

Obesity is characterized by an accumulation of adipose tissue that originates from increased production and activity of adipocytes. Adipocytes are formed by adipogenesis (5). During adipogenesis mesenchymal precursor cells differentiate into mature adipocytes under the influence of transcription factors like the CCAAT/enhancer-binding protein (C/EBP) gene family and peroxisome proliferator activated receptor-γ (PPAR-γ) (6). C/EBP-β and C/EBP-δ induce PPAR-γ, which regulates the stimulatory pathway of fat cell differentiation. In a positive feedback loop C/EBP-α and PPAR-γ then activate each other to maintain the differentiation status of the fat cells. Both the stimulation and the maintenance of adipogenesis are essential for fat production (7). Similarly, abnormal levels or impaired functionality of PPAR-γ and C/EBP transcription factors results in decreased development, maintenance and distribution of adipocytes. In mice, this was shown to lead to a decreased amount of adipose tissue(8). Additionally, PPAR- γ enhances lipid uptake and triacylglycerol storage. An important aspect of this cellular reprogramming includes reducing the capacity of lipid catabolising pathways such as β-oxidation. One approach to prevent lipid utilization during adipogenesis is to degrade mitochondria by a process called mitophagy. Limiting mitochondria ultimately preserves the adipocytes ability to generate and store lipids in the absence of an overly oxidative environment.

1.2 Obesity

Obesity is a worldwide epidemic that affects over 600 billion people (1). The World health organization (WHO) defines obesity as an excessive accumulation of adipose tissue with a body mass index (BMI) greater than or equal to 30 (2). In 2014, 11% of men and 15% of women aged 18 years and older were obese. Chronic obesity results in increased risks for severe health complications such as the metabolic syndrome, cardiovascular diseases, respiratory disorders, diabetes and cancer. Furthermore, obesity is associated with premature death, accounting for an estimated 3.4 million deaths per year (2, 3). The burden of obesity weighs tremendously on society with an estimated cost of $147 billion per year, or 9% of all annual medical expenses (4). The disability adjusted life years (DALYs), which is the sum of potential life years that are lost due to premature mortality and productive life years lost due to disability were estimated to be as high as 93.6 million in 2010 (1). With this growing epidemic of obesity and its associated health complications, there is an urgent

need to understand the underlying molecular mechanisms that cause this disease. This knowledge can be used to explore novel approaches to prevent or treat obesity, which can lead to a significant drop in the prevalence, which subsequently will lower medical costs. Development of such resources will not only be beneficial for the individual patient, but for the entire global society.

1.3 Mitophagy

Mitochondria are essential organelles that control cellular processes like cell death, cell growth and differentiation. They produce the adenosine triphosphate (ATP) molecules required for lipolysis and lipogenesis, β-oxidation and fatty acid (FA) synthesis in adipocytes (9). In concordance with their morphology, the cytoplasm of white adipocytes primarily consists out of a central lipid vacuole and there is little cytoplasmic space for other organelles including mitochondria (Fig. 1) (5, 10). During adipogenesis, the number of mitochondria decreases by a type of macro-autophagy known as mitophagy. This degradation of mitochondria is necessary for mature adipocytes to accumulate fat, while sustaining basal cellular functions (11). During the process of mitophagy, pre-adipocytes sequester their mitochondria in a double membrane structure, which is known as an autophagosome. This autophagosome delivers the entrapped mitochondria to lysosomes where they are degraded (12). In order to maintain a healthy mitochondrial network, organelles alternate between cycles of fission and fusion (Fig. 2) (13). Although both processes are necessary for maintaining bioenergetic requirements, mitochondrial fission is the one linked to the process of mitophagy (14). Mild defects in mitophagy and mitochondrial fission are associated with abnormal mitochondrial dynamics which may lead to metabolic and other diseases (10). Several independent groups showed that inhibition of mitophagy resulted in markedly changed phenotypes of white adipocytes (15, 16). These adipocytes exhibit an increased number of mitochondria and unusual morphological characteristics that resemble the phenotype of brown adipocytes (a class of adipocytes with high mitochondrial content). This atypical morphology is characterized by many small lipid droplets inside the cytoplasm rather than the single large

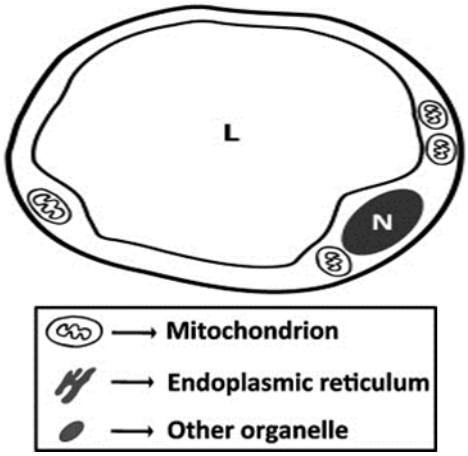

Figure 1: Mature white adipocyte with a central, unilocular, large lipid droplet that comprises almost the entire cytoplasm. Mitochondria are degraded during the formation of white adipocytes in a process known as mitophagy (10).

lipid droplet typically seen in white adipocytes. Furthermore, Singh *et al.* observed that adipocytes with an increased number of mitochondria fail to accumulate as much fat as their wild-type counterparts (17). These results provide new insights for regulating the size and cellular structures of adipose tissue in obese individuals. Another recent study showed that inhibition of mitophagy during the early stages of adipocyte differentiation arrests the process of adipogenesis (18). These findings support the essential role of mitophagy during adipogenesis through regulation of the number of mitochondria in mature adipocytes.

In vivo studies in which essential mitophagy genes were deleted show the beneficial effects of eliminating mitophagy on whole-body metabolism (15-17). These genes include autophagy gene 5 (Atg5), which encodes an essential protein for autophagy in adipocyte

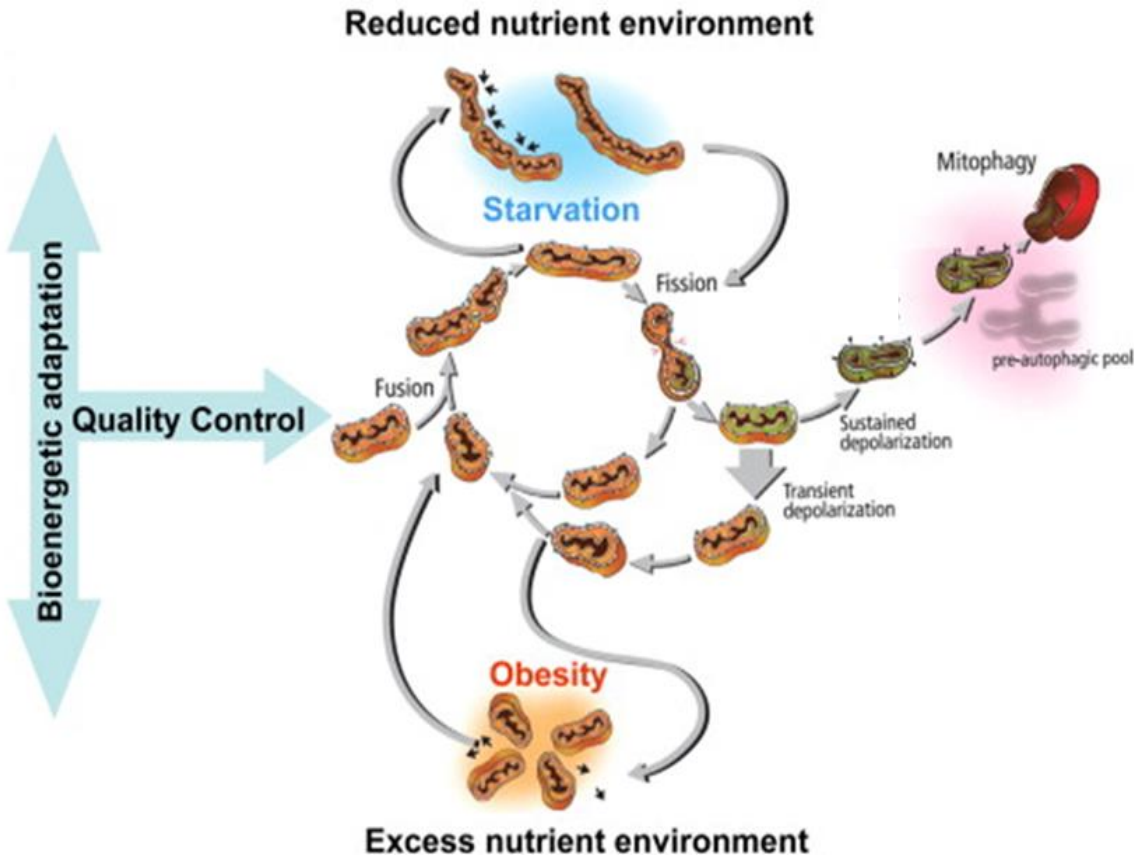

Figure 2: Mitochondria are dynamic organelles that undergo several cycles of fission and fusion during their lifetime. Fusion combines the components of two mitochondria, mixes and reorganizes them to keep a pool of healthy and heterogeneous mitochondria. Fission on the other hand splits mitochondria into two daughter organelles that may have different membrane potentials. Only healthy mitochondria will be allowed to continue through the fusion cycle, while depolarized, unhealthy mitochondria are silenced into a pool of pre-autophagic, solitary mitochondria. Obesity is a state of reduced bioenergetic efficiency, which causes uncoupling of respiration and increased fission of mitochondria (13).

differentiation, and Atg7, which encodes for an enzyme that is necessary for the autophagosome formation. Mutated mice, in which either Atg5 or Atg7 was specifically

deleted, exhibit reduced fat deposits, resistance to diet-induced obesity and increased insulin sensitivity. This can be explained by the increased number of mitochondria that are present in mitophagy-deficient adipocytes. This resulted in an elevation of β-oxidation and a subsequent decrease in free FA in plasma. A reduction in free FA concentration in plasma increases the insulin sensitivity of peripheral tissues. Although the process of adipocyte mitophagy has been intensively investigated, it is not yet known how mitophagy is initiated and how cells target specific mitochondria for destruction. Nevertheless, abnormal mitochondrial clearance impairs pre-adipocyte differentiation and alters the physiology of adipocytes, which may lead to metabolic diseases. One may presume that there must exist a coordination of cellular stress responses with mitochondria, to have optimal mitochondrial numbers in various tissues and cell types.

1.4 c-Jun N-terminal Kinase (JNK) function and activation

One of the central mediators of insulin resistance, obesity, and global cellular stress responses is the serine/threonine protein kinase, c-Jun N-terminal kinase (JNK). It was shown that inhibition of the JNK pathway improves insulin resistance and it has been suggested to be a crucial link between stress and metabolic diseases (19). JNK is part of the mitogen-activated protein kinase (MAPK) superfamily and is also known as the stress-activated protein kinase (SAPK) (20). Activation of JNK occurs through dual phosphorylation by MAPK kinases (MAPKK), which in turn get activated by MAPKK kinases (MAPKKK). These

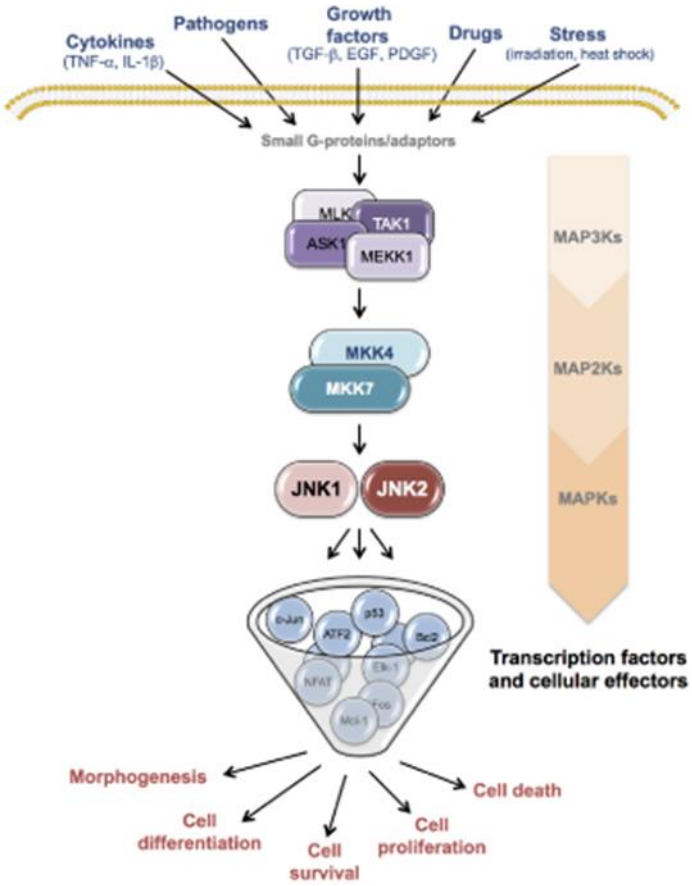

Figure 3: JNK is a stress-activated mediator that is part of the MAPK superfamily. In this figure the different steps of activation are displayed. Phosphorylation (encircled P) plays an important role in this activation cascade and in the response of JNK to environmental stimuli. Transcription factors are encircled in dark blue. JNK: c-jun N-terminal Kinase; MAPK: mitogen-activated protein kinase (3).

MAPKKK are responsive to stress stimuli, which can activate the signaling cascade that is critical for cellular responses to environmental stimuli (Fig. 3). Prolonged JNK activity results in pro-apoptotic transcription, phosphorylation of pro-apoptotic proteins and cell death (21). c-Jun is one of the transcription factors that is phosphorylated by JNK and this event promotes activator protein-1 (AP1) mediated transcription. AP-1 is known to play a role in differentiation, proliferation, and apoptosis (22). Significant evidence suggests that JNK signaling is a crucial event in the regulation of apoptosis. Moreover, mitochondrial translocation of JNK has been suggested to initiate the entire process of apoptosis (23). It was shown that at mitochondrial level, JNKs are responsive to reactive oxygen species (ROS), which are a byproduct of cellular respiration as well as a consequence of mitochondrial dysfunction (24) (Fig. 4). In addition, it is known that nutrient excess increases ROS due to incomplete mitochondrial FA oxidation. This contributes to impaired glucose signaling and decreased glucose oxidation, linking this pathway to type 2 diabetes (T2D) and obesity (25). Accumulating ROS will eventually cause a dissipation of the mitochondrial membrane potential, which in turn will lead to cytochrome C release, a hallmark of mitochondrial dysfunction. Early ROS induces apoptosis signaling regulated kinase 1 (ASK1), which is responsible for mitochondrial JNK translocation and the JNK response to oxidative stress. JNK signaling contributes to the production of more ROS during stress by inhibition of respiratory complex 1, which decreases the respiratory function. In this way, a positive feedback loop is initiated which changes the mitochondrial physiology during stress towards the promotion of ROS generation and self-destruction (24). Finally, JNK has been implicated in adipogenesis; wherein, the use of a small molecule JNK inhibitor was sufficient to

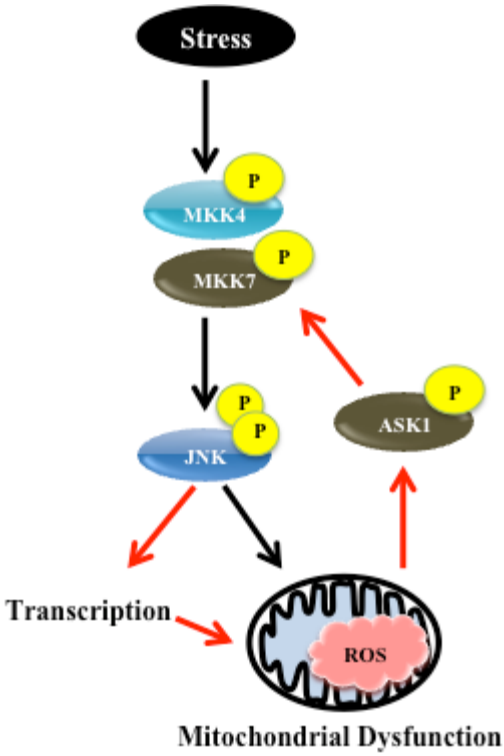

Figure 4: Mitochondrial JNK signaling is initiated by cellular stress. This primary response (black arrows) induces mitochondrial dysfunction and the amplification of ROS. This induces a secondary JNK signaling response that further exacerbates mitochondrial dysfunction through both nuclear and mitochondrial mechanisms (red arrows). MKK: MAPKK, Mitogen-activated protein kinase kinase; JNK: c-Jun N-terminal kinase; ROS: Reactive Oxygen Species; ASK1: apoptosis signaling regulated kinase 1

prevent adipogenesis (26). These data implicate the role of JNK in adipogenesis and obesity-related diseases.

1.5 Mitochondrial JNK Signaling

The relationship between JNK and mitochondria during adipogenesis has yet to be investigated; however, JNK has been shown to interact with the scaffold protein Sab (or SH3-binding protein 5, SH3BP5) on the outer mitochondrial membrane (OMM) and alter mitochondrial physiology. In an experiment where Sab was silenced in HeLa cells, JNK decreased on the mitochondria after being induced by stress. Silencing Sab resulted in less cytochrome C release, reduced ROS production during stress and increased cell viability (23). Therefore, it was speculated that mitochondrial translocation of JNK is dependent upon the ability of JNK to phosphorylate Sab. Interfering with the JNK/Sab interaction not only prevented JNK translocation to the mitochondria, but also the phosphorylation of B-cell lymphoma 2 (Bcl-2), which is also observed when knocking down JNK alone. Silencing Sab did not have an impact on the nuclear function or expression of JNK (23). Therefore, disruption of the JNK/Sab interaction at the OMM is a selective way of evaluating mitochondrial JNK signaling, without interfering in nuclear JNK signaling. The ability of JNK signaling to induce mitochondrial dysfunction may drive adipogenesis. Specifically, induction of mitochondrial stress may result in fragmentation of the mitochondrial network and degradation of damaged mitochondria by mitophagy.

1.6 Preliminary Studies

Preliminary data in our lab demonstrated that during adipogenesis the scaffold protein Sab promotes signal transduction events that regulate mitochondrial degradation. Specifically, silencing Sab expression or inhibiting the JNK/Sab interaction resulted in decreased adipose production in differentiated 3T3-L1 pre-adipocytes. Further, disrupting mitochondrial JNK signaling resulted in increased β-oxidation and reduced triglyceride levels in adipocytes. Inhibition of mitochondrial JNK signaling retained the oxidative metabolism and a mitochondrial density similar to undifferentiated pre-adipocytes. Finally, ectopic expression of Sab resulted in the fragmentation of the mitochondrial network in pre-adipocytes. Taken together these results demonstrate an essential role for mitochondrial JNK signaling in mitochondrial dynamics and adipogenesis.

However, Sab must be stabilized on the OMM in order to maintain the protein-protein interactions that regulate mitophagy. The stability of Sab may be controlled by post-translational modifications, potentially by N-terminal acetylation of lysine 6 (K6), a site

that has recently been identified in our lab. We propose that K6 acetylation increases the stability of Sab, leading to signal transduction events that promote mitophagy, which is necessary for the formation of adipocytes. Further evidence demonstrates that acetylation is linked to energy metabolism and it appears to be a regulatory mechanism for controlling the function and localization of mitochondrial proteins. Moreover, the cellular acetyl pool increases during adipogenesis (27). Taken together, these results suggest that mitochondrial metabolic changes in the developing adipocyte may influence mitophagy by modulating signal transduction pathways.

1.7 Experimental aims and approach

This project investigated the role of the scaffold protein Sab in mitophagy initiation and coordination during the process of adipogenesis. The knowledge generated out of this work may lead to novel approaches for the manipulation of adipocytes in order to prevent or treat obesity. The development of successful prevention and/or treatment programs will lead to a significant drop in the prevalence of obesity, its related co-morbidities, and medical costs.

We here suggest that K6 acetylation of Sab increases its stability, and in this way preserves Sab's ability to promote mitophagy during adipogenesis. We conducted experiments to test if Sab is indeed acetylated at K6 and to identify the main acetyltransferases and deacetylases that are responsible for this posttranslational modification. Furthermore, we predict that a non-acetylatable Sab mutant (K6A) will reduce mitophagy. In addition, the relation between Sab acetylation and the process of adipogenesis was explored. To challenge our hypothesis, the following independent objectives were used.

1. Examine Sab expression and the presence of K6 acetylation on Sab at different time points of adipogenesis, using the 3T3-L1 mouse pre-adipocyte cell line as a model. This is a well-established cell-line to study the process of mitophagy during adipogenesis. These white pre-adipocytes will be differentiated into adipocytes using established techniques. K6 on Sab was previously shown to contain a specific acetylation site motif and no other lysines have been predicted to be acetylated by bioinformatics. Sab will be isolated from the mitochondria at different phases of adipogenesis, and subjected to western blot analysis, or mass spectrometry analyses to evaluate Sab abundance and post-translational modifications.
2. Explore the possible mechanisms that control Sab stability and expression, by using different differentiation stimuli and induction of metabolic confusion.

3. Determine the impact of K6 mutation on mitophagy and adipogenesis. Using site-directed mutagenesis, amino acid residues of K6 were changed to emulate acetylated and non-acetylated states of Sab. This was established by changing lysine to glutamic acid (K6E mutant) for the acetylated state, and lysine to alanine (K6A mutant) for mimicking the non-acetylated state. These Sab-mutant cDNAs were expressed in 3T3-L1 cells to study their impact on mitochondrial morphology. With this experiment, a link between K6 acetylation of Sab and mitophagy regulation in adipocytes was investigated for the first time.
4. Identification of the main acetyltransferases and deacetylases that are responsible for the post-translational modification of Sab by silencing major protein deacetylases. With this experiment the impact of Sab acetylation on protein level and stability was explored, which elucidates some of the mechanisms that control mitophagy during adipogenesis.

Chapter 2
Materials and Methods

2.1 Cell Culture

3T3-L1 (CL-173) mouse pre-adipocytes and NIH-3T3 cells (CRL-1658) (American Type Tissue Culture, Manassas, VA) were grown under standard cell culture conditions, at 37°C and under 5% CO_2, in Dulbecco's Modified Eagle Medium (DMEM) supplemented with high glucose-GlutaMAX (Life Technologies, Inc. Carlsbad, CA) and 10% fetal bovine serum (FBS, Denville Scientific Inc., South Plainfield, NJ) or newborn calf serum (NCS, Denville Scientific Inc., South Plainfield, NJ), 1% penicillin, 1% streptomycin (Life Technologies, Inc.) and 0.1% plasmocin (Invivogen, San Diego, CA). Cells used for experiments were between passages 5 and 25 for all studies.

2.2 Differentiation

Adipocyte differentiation was performed in 35-mm dishes (Fisher Scientific). Cells were seeded at a concentration of 6 x 10^5 cells per dish. To differentiate 3T3-L1 pre-adipocytes into mature adipocytes, a 14-day protocol was used as described by Zebisch e*t al.* (Fig. 5) (28). Medium was changed every other day and during the first 3 days the cells grew in basal medium I (BM I = DMEM + 10% NCS + 1% P/S + 0,1% plasmocin prophylactic). The day of seeding was defined as day 0, and on day 1, when cells were confluent, the medium was replaced. On day 3 (48 hours after confluency) the medium was changed to differentiation medium I (DM I), consisting out of basal medium II (BM II = DMEM + 10% FBS + 1% P/S + 0.1% plasmocin) plus four chemicals required for differentiation: insulin (1 µg/mL), dexamethasone (DEX, 0.25 µM), iso-butylmethylxanthine (IBMX, 0.5 mM), and rosiglitazone (2 µM). On day 5, DM II or maintenance medium was added to the cells, which consisted out of BM II supplemented with insulin (1 µg/mL). On day 7, BMII was added to the differentiating cells for the remainder of the differentiation. Around this time point, lipid droplets became visible which showed an increase in number and size during the following days of the protocol. This medium was refreshed on days 8, 10, 12 and 13. On day 14 of the differentiation protocol, 3T3-L1 cells were fully differentiated and showed the histological characteristics of mature fat cells with various sizes of intracellular lipid droplets.

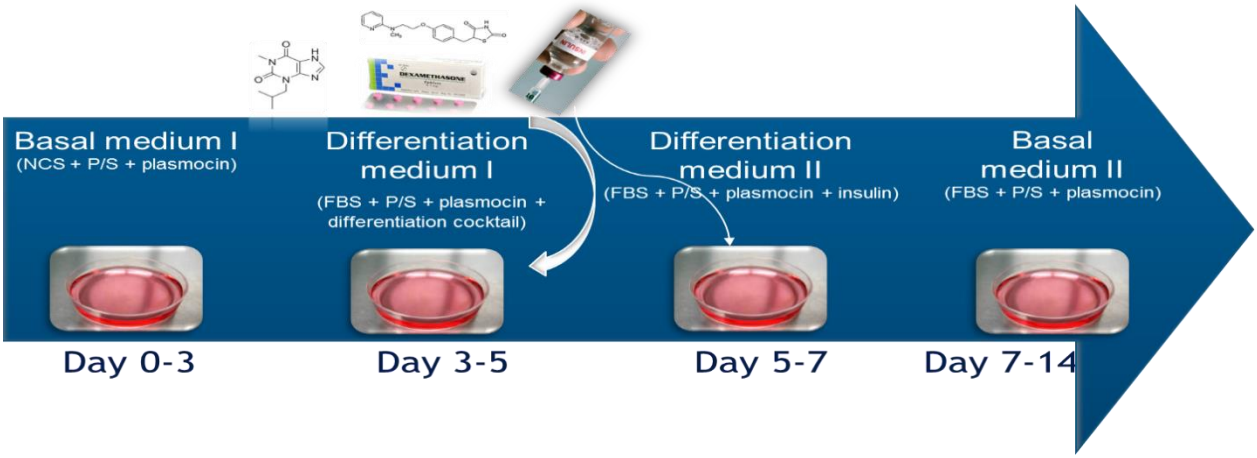

Figure 5: Two-week protocol according to Zebisch *et al.* (28). After growing the cells in DMEM + FBS until confluency in a T-175 flask, the 3T3-L1 pre-adipocytes were plated in 35-mm dishes containing DMEM + NCS (BM I). After plating on day 0, the medium was refreshed on day 1 and replaced with DM I on day 3. This medium contains the four differentiation inducers insulin (1 µg/mL), dexamethasone (0.25 mM), IBMX (0.5 M) and rosiglitazone (2 µM). At day 5 the medium was changed to DM II that contains only insulin. Finally on day 7 BM II was introduced and this medium was refreshed on day 8, 10, 12 and 13. On day 14 cells were fully differentiated into mature adipocytes. DMEM: Dulbecco's Modified Eagle Medium; FBS: Fetal bovine serum; NCS: Newborn calf serum; BM I: Basal medium I; DM I: Differentiation medium I; IBMX: Iso-butylmethylxanthine; DM II: Differentiation medium II; BM II: Basal medium II.

2.3 Preparation of protein lysates

To collect proteins for western blotting and other experiments, cells were lysed with 100 µL of Li-Cor lysis buffer (20 mM Tris-HCl (pH 7.5), 150 mM NaCl, 1 mM Na_2EDTA, 1 mM EGTA, 1% Triton X-100), supplemented with HALT® protease and phosphatase inhibitor cocktails (ThermoFisher Scientific, Inc., Waltham, MA), after washing them twice with 1 mL of ice-cold phosphate-buffered saline (PBS) or hank's balanced salt solution (HBSS). Cells in lysis buffer were incubated for 5 minutes at 4°C while rocking gently. After this, cells were scraped from the surface with a cell scraper (Fisher Scientific) and transferred to 1.5 mL micro-centrifuge tubes (ThermoFisher Scientific). Subsequently the lysates were sonicated for 30 seconds, cooled down in ice for 5 minutes and centrifuged at 21 130*g for 15 minutes at 4°C. The supernatant containing the proteins was collected in new 1.5 mL micro-centrifuge tubes and then stored at -80°C for subsequent analysis.

The time points at which the cells were collected were dependent on the experiment and are indicated in the result section (chapter 3). For the differentiation experiments cells were collected at each day of the differentiation protocol at the same time every day. On the days the medium was changed, cells were collected before the medium change was performed.

For the 48-hour experiments using the differentiation agents, cells were plated in 35-mm dishes and grown until confluency was reached. After approximately 24 hours the individual differentiation inducers or the different media sources without additional

chemicals were added to the cells. 48 hours later, all cells were collected as described above and stored until further analyses.

2.4 Protein quantification

Protein concentrations of lysed samples were determined using the bicinchoninic acid (BCA) assay. In this assay, a color change from green to purple is proportional to the protein concentration in the sample. This change is measured via a colorimetric technique using the Synergy H1 plate reader (Bio-Tek, Lincoln) which simultaneously measures the coefficient of variance (CV). Samples were plotted against nine standard samples of known protein concentration. Samples and standards (25 µl/well) were loaded in duplicate in a 96-well plate (Corning Incorporated, NY). After addition of the working reagent (200 µl/well), the plate was wrapped into plastic foil and incubated at 37°C for 30 minutes before scanning. CVs lower than 20% were considered acceptable.

2.5 Western blot analysis

Western blotting was performed using standard methods. The necessary concentrations to run western analyses were calculated to be at least 25 µg/well. A minimum of 2 replicates per experiment was used. The protein lysates were mixed with 6X loading buffer and denaturated by heating them at 95°C for 5 minutes. Subsequently the samples were cooled in ice for 10 minutes and loaded on the gel to be resolved by sodium dodecyl sulfate polyacrylamide gel electrophoresis (SDS-PAGE) at 100 volts. The separated proteins were then transferred to nitrocellulose or polyvinylidene fluoride (PVDF) membranes using either a wet or a dry (Transblot Turbo, Bio-Rad, California) transfer depending on the primary antibody to be used (See Section 2.5.1 Antibodies). After transfer of the proteins to the membranes, they were incubated with 1X tris-bufferd saline (TBS) blocking buffer (20mM Tris-HCl, 137mM NaCl, pH 6.7) supplemented with the blocking agent 5% bovine serum albumin (BSA, Fischer Scientific, Pittsburgh, PA), or non-fat milk depending on the primary antibody to be used, for a minimum of 1h at room temperature (RT) while gently rocking. Overnight blocking was always performed in the cold room at 4°C. After blocking of the membranes, incubation with the primary antibodies was performed at the proper dilutions in 0.1 % TBS-T blocking buffer (1X TBS with 0.1% Tween-20 and 5% BSA or non-fat milk) for 2.5 hours at RT or overnight at 4°C. Five-minute washes with TBS-T were repeated three times for each membrane before incubation with the secondary fluorescent-conjugated antibodies (anti-Rabbit, DyLight-680 conjugate and anti-Mouse DyLight-800 conjugate). The secondary antibodies were added at a dilution of 1:20000 for 45 minutes at

RT while gently rocking. After 3 washes, the western blots were developed for fluorescence detection with the Odyssey scanner (Li-Cor Biosciences).

2.5.1 Antibodies

The primary antibodies used for western blot analysis were purchased from multiple vendors. The antibody used to detect Sab (H00009467-M01) was purchased from Novus Biologicals (San Diego, CA). The following antibodies were purchased from Cell Signaling Technologies (Danvers, MA): Phospho-JNK (#4668), JNK/SAPK (#9258), 5' adenosine monophosphate-activated protein kinase α (AMPKα, #2603), Phospho-AMPKα (#2535), PPARγ (#2443), Sirtuin 1 (SIRT1) (#2496), α-Tubulin (#3873), Atg5 (#8540), Atg7 (#3558), mammalian target of rapamycin (mTOR #2983), Phospho-Raptor (#2083), Cytochrome c oxidase, or complex IV (COX-IV, #4850), Phospho-p38 (#9216), and Phospho-p42/p44 (#4370). Mitochondrial transcription factor A (mtTFA, sc-376672) was purchased from Santa Cruz Biotechnology, Inc. (Dallas, TX). Secondary antibodies were purchased from Li-Cor Biosciences, Inc. (Lincoln, NE) and Cell Signaling Technologies. Li-Cor bioscience antibodies were anti-rabbit IR-Dye 680RD (#925-680710) and anti-mouse (#926-32211). Secondary antibodies from Cell Signaling Technologies were anti-rabbit DyLight-680 (#5366) and anti-mouse DyLight-800 (#5257).

2.6 BSA-Fatty Acid Conjugation and Treatment

Palmitate must be conjugated to BSA in order to be water-soluble and to facilitate cellular uptake. In order to prepare BSA-palmitate, the two reagents had to be combined at a 6:1 molar ration using the approach described below. Briefly, 2.267 g of ultra FA free BSA (Sigma-Aldrich, St. Louis, MO) was dissolved in 100 mL warm NaCl (37^{o}C) while stirring on a hot plate warmed to 37^{o}C. Once the BSA was completely dissolved, it was filter sterilized. Next, 50 mL of BSA was combined with 50 mL of 150 mM NaCl. Palmitate (30.6 mg) was then added to the BSA-NaCl solution, which was heated to 70^{o}C. After this the solution was cooled to 37^{o}C and stirred until the palmitate was completely dissolved. The pH was adjusted to 7.4 with 1N NaOH. The solution was aliquoted in glass vials and stored at -20^{o}C for future use.

As a control, linoleic acid was also conjugated to BSA using an identical approach. Linoleic acid does not cause nutrient excess in mammalian cells and would be used as a negative control. BSA alone is used as a vehicle control for both palmitate and linoleic acid.

Palmitate experiments were performed in the same way as the differentiation experiments until day 3. At day 3 BSA-palmitate, BSA-linoleic or BSA (Seahorse bioscience, North

Billerica) was added to the cells at different concentrations. Cells were lysed at different time points (0, 0.5, 1, 2, 3, 4, 8, 12, or 24 hours).

2.7 Plasmid Purification and Site-directed Mutagenesis

The plasmid pLOC:Sab was acquired from the laboratory of Dr. Philip LoGrasso at the Scripps Research Institute. The plasmid was stored in DH5α *E.coli*, which were grown in Lauria Broth (LB) supplemented with 50 mg/mL ampicillin. For Maxi-preps (~1 mg) of plasmid DNA, bacteria were cultivated overnight and harvested by centrifugation. DNA was purified from bacteria using the Qiagen Maxi-prep kit protocol (Valencia, CA). Purified plasmid DNA was resuspended in water and quantified by spectrophotometry.

Next, the DNA was subjected to site-directed mutagenesis according to the Phusion Site Directed Mutagenesis kit protocol which was purchased from Fisher Scientific. Briefly, 1 ng of plasmid DNA was incubated with specialized primers encoding mutations of the codon for K6 of Sab in the presence of a high fidelity DNA polymerase. PCR was then used to amplify the DNA containing the mutation, and the template DNA was degraded by adding DpnI resistriction enzyme to the completed reaction to destroy methylated (not newly synthesized) plasmid DNA. The mutations were confirmed by DNA sequencing services provided by the Scripps Research Institute.

2.7.1 Primers

Below are the primers that were used to mutate the pLOC:Sab plasmid in order to alter the K6 codon:

F.Sab:K7E:1-33: 5'-ATGGACGCGGCACTG**G**AGCGGAGCCGCTCGGAGGAG-3'

R.Sab:18-1: 5'-CCCCTTCAGTGCCGCGTCCAT-3'

F.Sab:K7A: 5'-ATGGACGCGGCACTG**GC**GCGGAGCCGCTCGGAGGAG-3'

Sequencing primers were provided by Open Biosystems.

2.8 Transfection

The pLOC:Sab plasmids were transfected into 3T3-L1 pre-adipocytes using the FugeneHD transfection reagent (Promega, Madison, WI). Briefly, 1μg of plasmid DNA was combined with 18μL of FugeneHD reagent in serum free medium for 20 minutes at RT. The transfection complex was then added to the cells for 8 hours under normal cell culture conditions. After 8 hours, media was exchanged to provide cells with fresh media free of liposomes. Sab expression was monitored at 48 hours and 72 hours post-transfection. Sab

expression was determined using western blot analyses described above. An identical transfection approach was used for the pHalo:Sab vector described below.

2.9 Fluorescent Microscopy

To determine if Sab was properly localized within the 3T3-L1 pre-adipocyte, we employed immunofluorescent microscopy. Cells were seeded at a density of 2.5 x 10^5 cells in a 35-mm plate with a German-glass bottom suitable for microscopy work. The cells were transfected as described above and analyzed for Sab expression using western blot analysis. Briefly, cells were fixed in 4% paraformaldehyde (25 minutes at RT) at 48 and 72 hours post-transfection. Next, the cells were permeabilized with 0.1% Triton X-100 in 1X TBS for 30 minutes at RT. The cells were then quenched with 5 mM glycine, and blocked using 1X TBS-T supplemented with 5% BSA for 1 hour. The primary antibody for Sab was added in 1X TBS-T with 5% BSA and incubated for 4 hours at RT. The cells were washed in 1X TBS-T for 5 minutes at RT while gently rocking. The secondary antibody anti-mouse AlexaFluor 488 (Cell Signaling Technologies, #4408) was added and incubated for 1 hour at RT while gently rocking. The cells were then imaged using a 488 filter on the Olympus Fluorescent Microscope system at the Scripps Research Institute.

2.10 Identification of Sab acetylation sites with mass spectrometry

To determine if Sab was indeed acetylated on the N-terminal lysines, Sab was cloned into a HaloTag (Promega) containing the vector for purification and analysed by mass spectrometry. The pHalo:Sab vector was obtained from the Chambers lab freezer storage. The plasmid was transfected into 3T3-L1 pre-adipocytes as described above. The cells were then subjected to differentiation and other stresses as described in the results section (chapter 3). Following treatment, the cells were lysed using homogenization and sonicated in PBS supplemented with the deacetylase, and acetyltransferase inhibitor butyric acid (10 mM) along with protease and phosphatase inhibitor cocktails. Sab was purified from the lysates using an affinity column containing the HaloLigand (Promega) according to the manufacturer's protocol. Proteins were resolved by protein gel electrophoresis, and a single band at ~70kDa was visualized with silver stain and excised with a scalpel. The gel band was provided to the Scripps Research Mass Spectrometry Core for analysis. Briefly, the protein was extracted from the gel and subjected to enzymatic (trypsin) digestion. Next, tandem mass spectra of peptides from the protein sample were obtained using nano-electrospray injection tandem mass spectrometry. Two μL of sample was loaded into the injector, and subsequently analyzed. Parent ions collected during the analysis were

examined for those corresponding to the same mass-to-charge ratio of K6 acetylated Sab. Secondary ion analysis was used to confirm. Also, an anti-acetyl-lysine antibody (Cell Signaling Technology, #9441) was used to detect the presence of acetylation on Sab.

2.11 Gene silencing of sirtuins

To determine if the sirtuin family of deacetylases regulates Sab acetylation under normal conditions in 3T3-L1 pre-adipocytes, small interfering RNAs (siRNAs) were used to silence the expression of sirtuins 1-5 individually. The siRNAs used for this experiment were provided by the Cell-Based Screening Core at the Scripps Research Institute, Florida campus. Briefly, cells were plated at a density of 2.5×10^5 cells per 35-mm plate. When the cells reached approximately 60% confluency, a mixture of 100 ng siRNA, 15 μL Hi-Perfect reagent (Qiagen), and 85 μL serum free media were added to the culture for 72 hours. Silencing of the respective sirtuins was assessed by western blotting. The optimal siRNAs were then provided to us for our investigations. We incubated the cells with siRNAs for 24 hours, and then transfected the cells with the pHalo:Sab vector for 72 hours. Sab was purified and analyzed for acetylation as described immediately above.

2.12 Statistics and Replicates

To determine the statistic validity for individual observations, a series of biological replicates were employed. No fewer than three biological replicates were used for each observation. For mass spectrometry analyses, at least six purifications were analyzed. For each assay, a minimum of two experimental replicates were employed, and plate based assays contained at least five replicates per sample. Statistical significance between conditions of the same experiments were obtained using the standard Student's t-test. Significance between experiments was determined using the Tukey's ad-hoc test. Statistics for mass spectrometry experiments were calculated using the MSStat software package by the personnel of the Scripps Research Institute's proteomics core facility.

Chapter 3
Results

3.1 Sab expression increases during adipogenesis prior to mitophagy genes

To determine if Sab expression was selectively enriched during the process of adipogenesis, we differentiated mouse 3T3-L1 pre-adipocytes into mature adipocytes using a well-established 14-day protocol. On each day of the differentiation process, 3T3-L1 cells were lysed and proteins were isolated and quantified. We then monitored the levels of expression using western blot analysis (Fig. 6). We found that Sab expression was initially low during early differentiation, and elevated quickly during days 3, 4, and 5 (Fig. 6A). The Sab levels remained elevated on days 6 and 7 of differentiation, and after this the concentration of Sab decreased during the remainder of the 14-day time course (Fig. 6A). To examine how Sab expression paralleled with the induction of genes involved in adipogenesis, we used western blot analysis to detect the relative abundance of adiponectin, fatty acid binding protein 4 (FABP4), and PPARγ. We found that adiponectin, FABP4, and PPARγ all increased very early during adipogenesis and were sustained for the remainder of adipogenesis (Fig. 6B). Next, we examined the levels of two proteins involved in autophagy Atg5 and Atg7. It was found that both Atg5 and Atg7 were elevated after day 6 of differentiation (Fig. 6C). Tubulin was used as a loading control to demonstrate that similar amounts of protein lysates were loaded into each sample well, while COX-IV was used as a mitochondrial loading control to assure equivalent amounts of mitochondria were present (Fig.6D). The fluorescent westerns were quantified using the ImageStudio® software from Li-Cor Biosciences (Fig. 6E). These results demonstrate that Sab is differentially expressed during adipogenesis.

3.2 Sab expression parallels JNK activation during adipogenesis

Sab was previously identified to be a scaffold for JNK; therefore, we examined the relative abundance of active (phosphorylated) JNK and total JNK during adipogenesis. Phospho-JNK levels increased on day 3 of adipogenesis and remained high until day 5; following day 5 Phopho-JNK levels returned to basal levels (Fig. 7A). Total JNK levels did not appear to change during adipogenesis (Fig. 7B). To examine the possible contributions of other MAPKs, the phosphorylation and abundance of p38 and extracellular-signal-regulated kinase (ERK) species was also measured. The levels of phospho-p38 increased after day 5 of differentiation, and then returned to basal levels on day 7 (Fig. 7C). Basal p38 levels

remained unchanged (Fig. 7D). Phospho-ERK levels increased at day 3 and remained elevated until day 7 (Fig. 7E), total ERK levels were unchanged (Fig. 7F). Tubulin was used as a loading control (Fig. 7G).

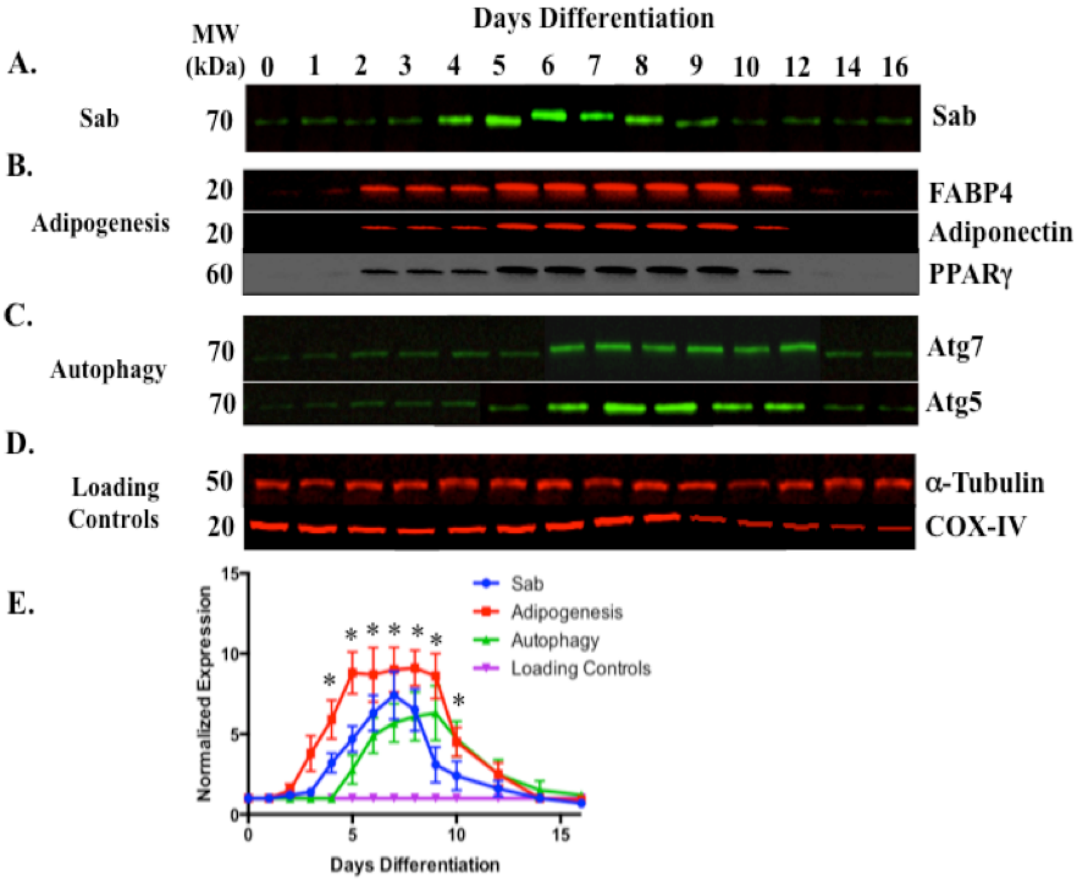

Figure 6: Sab is differentially expressed during differentiation of 3T3-L1 pre-adipocytes. To evaluate if and when Sab expression changed during adipogenesis, 3T3-L1 pre-adipocytes were differentiated into mature adipocytes over 14 days. **(A)** Cells were lysed and proteins were harvested on days 0, 1, 2, 3, 4, 5, 6, 7, 8, 9, 10, 11, 12 and 14. The cell lysates were assesses for Sab expression using western blot analysis. **(B)** Sab expression compared to the expression of adipogenic proteins FABP4, adiponectin, and PPARγ. **(C)** Sab expression compared to the expression of autophagic proteins Atg7 and Atg5. **(D)** Tubulin was used as a cellular loading control, while COX-IV was used as an index for mitochondrial proteins. **(E)** Sab expression was normalized to COX-IV and then to tubulin using the ImageStudio® software, while other proteins were normalized to tubulin. These results were plotted on an X-Y axis. Statistical significant changes in Sab levels are indicated by (*) and were calculated using the Student's t-test (p-value <0.005). FABP4: Fatty acid binding protein 4; PPARγ: Peroxisome proliferator activated receptor-γ; Atg: Autophagy gene; COX-IV: Cytochrome c oxidase, or complex IV.

The western blots were quantified by normalizing the fluorescence of each phospho-protein signal to the total control and then to the loading control (Fig. 7H). This provided a uniform background for phospho-protein changes with respect to total protein and loading control signals. These data demonstrate that MAPKs become activated at distinct times during adipogenesis.

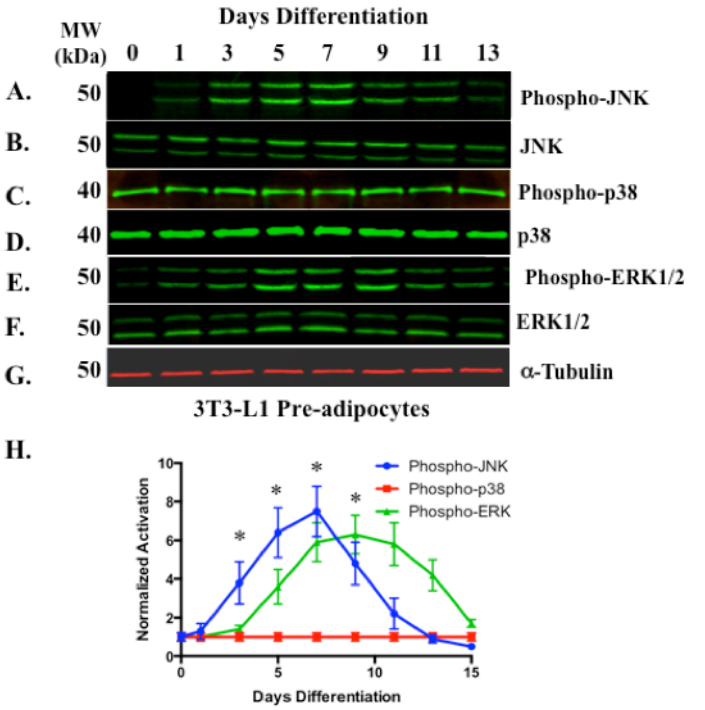

Figure 7: MAPKs are activated at distinct times during 3T3-L1 differentiation. 3T3-L1 pre-adipocytes were differentiated as describe in the *Materials and Methods*. Cells were lysed on days 0, 1, 3, 5, 7, 9, 11, and 13. The cells were analyzed for the presence of active (phosphorylated) MAPKs. Phospho-JNK **(A)** and total JNK **(B)** were measured by western blot analysis, as were Phospho-p38 **(C)**; total p38 **(D)**; Phospho-ERK1/2 **(E)** and total ERK1/2 **(F)**. The levels of phospho-MAPKs were normalized to total MAPK, followed by normalization to tubulin **(G)**. The normalized levels of active MAPKs were calculated using the ImageStudio® software and plotted on an X-Y axis **(H)**. A Student's t-test was used to determine statistical significant changes in activation of JNK and ERK1/2; significance is indicated by (*) (p-value <0.005). MAPKs: Mitogen-activated protein kinases; JNK: c-Jun N-terminal kinase; ERK: Extracellular-signal-regulated kinase.

3.3 Sab expression does not change by individual adipogenesis agents

To evaluate which adipogenic agent was affecting Sab levels in differentiating 3T3-L1 pre-adipocytes, cells were grown to confluency and then treated for 48 hours with the same dose of insulin, DEX, IBMX, or rosiglitazone used for differentiation. First, the serum change that occurs during 48 hours of differentiation was investigated. 3T3-L1 cells treated with NCS containing media or FBS containing media did not present a detectable change in Sab expression (Fig. 8A). Next, we evaluated the impact of each differentiation agent on Sab expression. Treatment with 1 µg/mL insulin for 48 hours did not have any impact on Sab expression (Fig. 8A). Cells treated with 0.25 µM DEX for 48 hours, showed no change in Sab levels (Fig. 8B). After 48 hours of exposure to 0.5 mM IBMX, there was no change observed in Sab expression (Fig. 8C). Finally, treatment with 2 µM rosiglitazone also did not have an impact on Sab levels (Fig. 8D). Again, tubulin was used as a loading control (Fig. 8A). To determine if the change in Sab expression could be attributed to the switch of serum from NCS to FBS, the 3T3-L1 cells were grown to confluency and exposed to NCS or FBS containing media for 48 hours. Changing the media to FBS for 48 hours did not impact Sab expression significantly (Fig. 8A), nor did maintaining the cells in NCS containing media for 48 hours (Fig 8B). The same trends were observed in the parental line NIH-3T3, which was investigated in order to rule out 3T3-L1 specific effects (Fig. 9). Changing the serum from NCS to FBS in the NIH-3T3 fibroblasts did not impact Sab

expression (Fig. 9A). Furthermore, the addition of individual differentiation agents (1 µg/mL insulin, 0.25 µM DEX, 0.5 mM IBMX, or 2 µM rosiglitazone) did not significantly alter Sab expression after 48 hours (Fig 9B). These data suggest that Sab levels are affected by the cumulative physiological state induced by the differentiation agents.

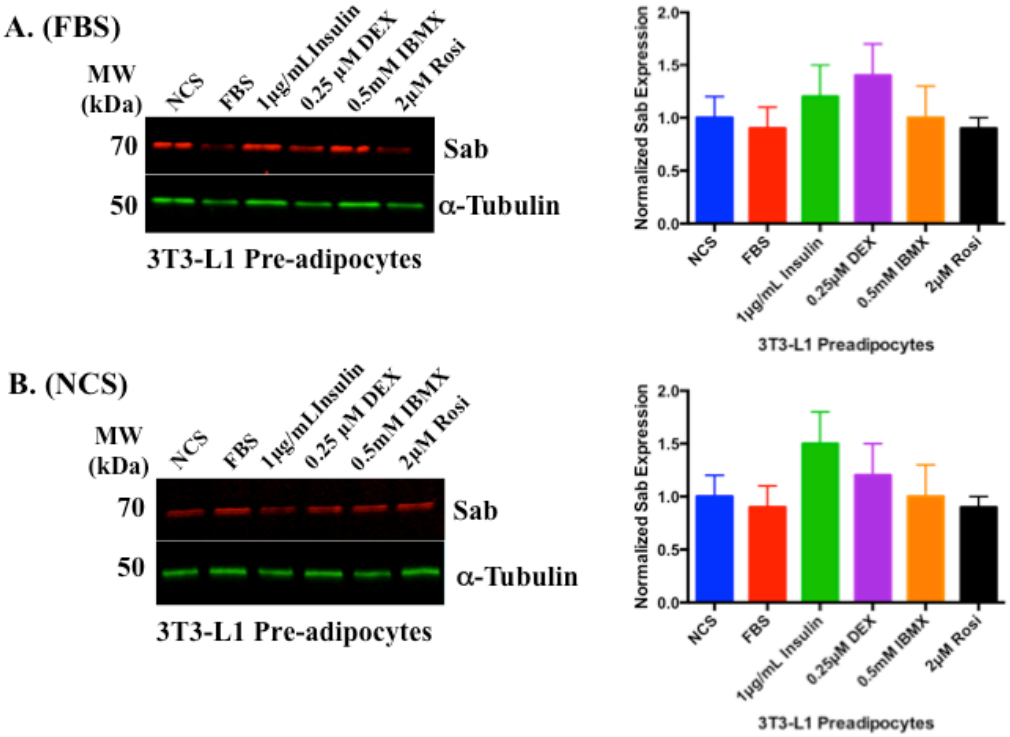

Figure 8: Serum and individual differentiation agents do not impact Sab expression in 3T3-L1 cells. (A) To emulate differentiation conditions, 3T3-L1 pre-adipocytes were grown to confluency, and after 48 hours, the cells were treated with media supplemented with NCS, media supplemented with FBS, or media with FBS and either 1 µg/mL insulin, 0.25 µM DEX, 0.5 mM IBMX, or 2 µM rosiglitazone. After an additional 48 hours, the cells were lysed and Sab levels were assessed by western blot analysis (left). Sab levels were normalized to tubulin levels using the ImageStudio® software (right). **(B)** To determine if pre-adapting the cells to NCS may amplify the effects of differentiation agents, cells were grown in media supplemented with NCS until confluency. The cells were maintained in media with NCS for 48 more hours, and then treated with media supplemented with NCS, media supplemented with FBS, or media with FBS and either 1 µg/mL insulin, 0.25 µM DEX, 0.5 mM IBMX, or 2 µM rosiglitazone for an additional 48 hours. Sab expression was assessed by western blot analysis (left) and quantified (right) as described immediately above. There were no statistical significant changes in Sab expression, data were evaluated using a Student's t-test for FBS and NCS experiments. Data between FBS and NCS experiments was analyzed using the Tukey's honest difference test. NCS: Newborn calf serum; FBS: Fetal bovine serum; DEX: Dexamethasone; IBMX: Iso-butylmethylxanthine.

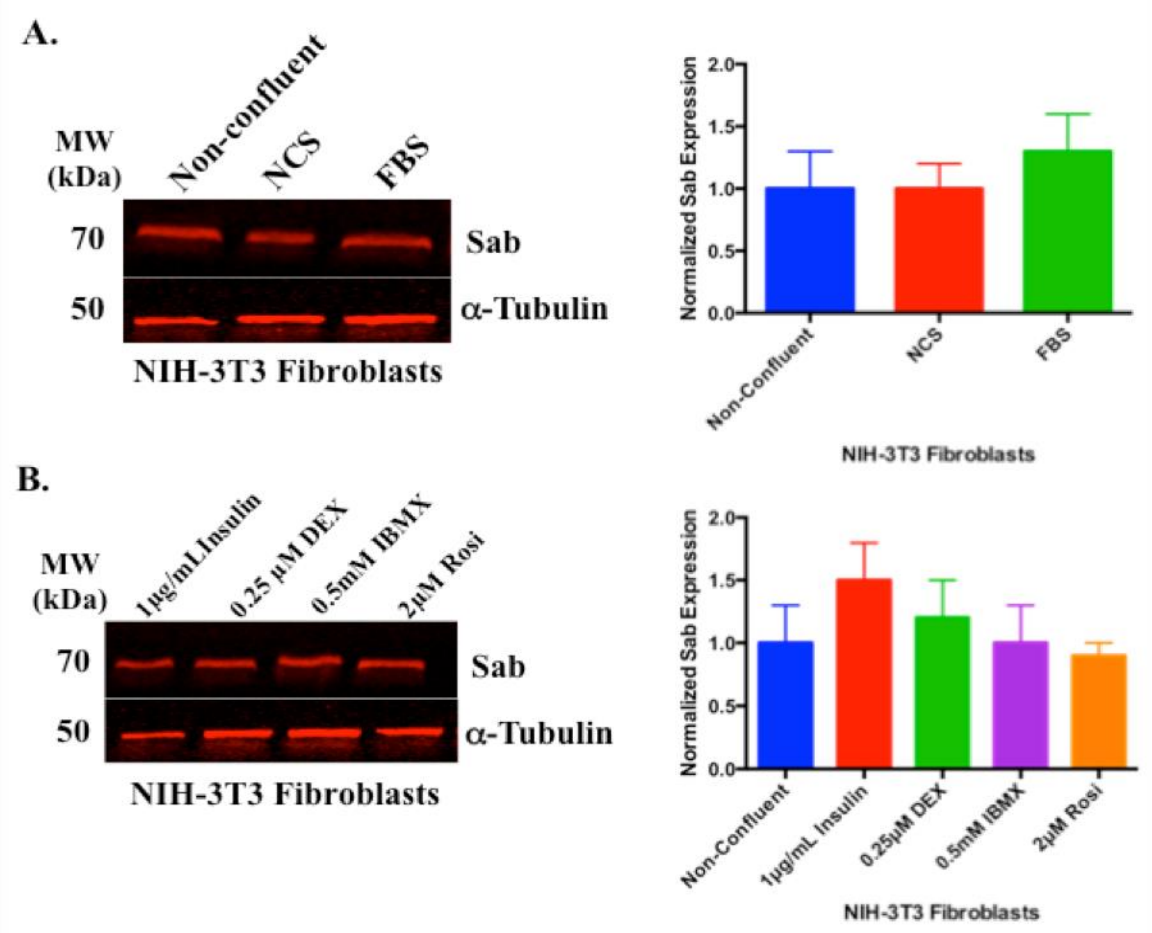

Figure 9: Differentiation agents do not impact Sab expression in parental NIH-3T3 fibroblasts. (A) Parental NIH-3T3 fibroblasts were grown to 80% confluency and then the media was changed to media supplemented with NCS or FBS. After 48 hours, the cells were lysed, and the abundance of Sab was assessed by western blot analysis (left). Sab levels were normalized to tubulin and quantified using the ImageStudio® software (right). **(B)** NIH-3T3 fibroblasts were also subjected to treatment with either 1 μg/mL insulin, 0.25 μM DEX, 0.5 mM IBMX, or 2 μM rosiglitazone for 48 hours. Sab expression was analyzed as described above. There were no statistically significant changes as determined by the Student t-test and Tukey's honest difference test. NCS: Newborn calf serum; FBS: Fetal bovine serum; DEX: Dexamethasone; IBMX: Isobutylmethylxanthine.

3.4 Sab expression increases by nutrient excess

The culmination of the differentiation of 3T3-L1 cells is the induction of fatty acid synthesis and lipid production, a state often referred to as nutrient excess. Nutrient excess can be induced by the addition of palmitate to cells to emulate increased nutrient availability. For palmitate to gain access to cells, it must be conjugated to BSA to improve water solubility and cellular penetration. We synthesized BSA-conjugated palmitate (BSA-palmitate) for our studies.

We also synthesized BSA-linoleic acid as a negative control, a plant-based fatty acid that does not trigger nutrient excess responses. Further, BSA alone was used as a vehicle control for BSA-dependent effects in cells.

Palmitate was added to cells using both acute and chronic exposures. For acute exposures, 3T3-L1 cells were grown to confluency, and after 48 hours treated with either 0.1 mM or 0.4 mM BSA-palmitate for up to 8 hours. During the 8-hour time course Sab expression was increased at the 4-hour time point and this continued up to the 8-hour time point (Fig. 10A). No change is Sab expression was observed for 3T3-L1 cells treated with 0.1 mM and 0.4 mM linoleic acid for 8 hours (Fig. 10B), nor were any significant changes in Sab abundance observed in cells treated with BSA-alone (Fig. 10C). Tubulin was used as a loading control (Fig. 10A-C).

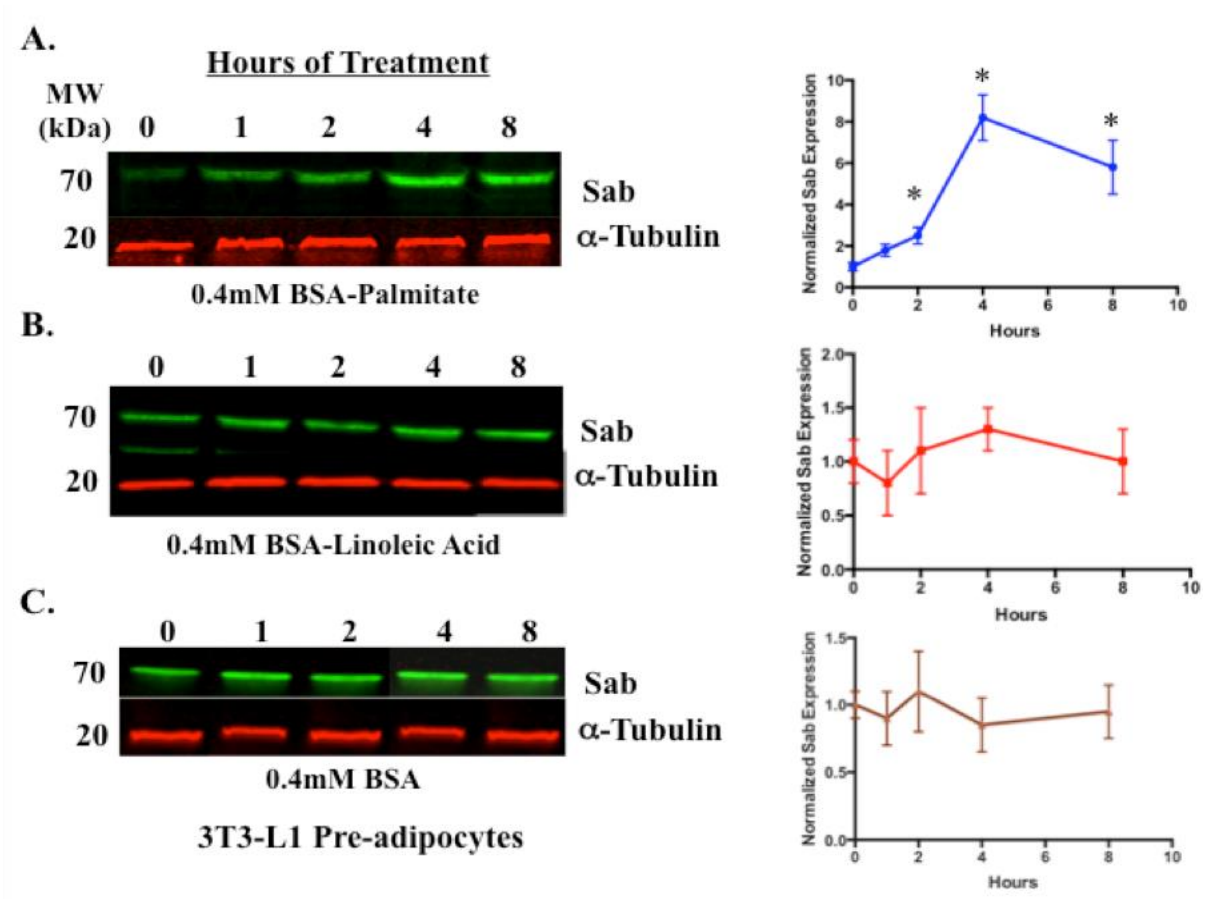

Figure 10: Acute nutrient excess stimulates Sab accumulation in 3T3-L1 pre-adipocytes. 3T3-L1 pre-adipocytes were grown to confluency and then treated with 0.4 mM BSA-palmitate **(A)**, BSA-linoleic acid **(B)**, or BSA alone **(C)** for 8 hours. Cells were lysed at the indicated time points and Sab levels were measured by western blot analysis. Tubulin was used as a loading control. Western blots were quantified using the ImageStudio® software. Sab was normalized to tubulin to account for loading and to normalize to a stably expressed protein. Quantified westerns are positioned to the right of their respective blots in each figure. Statistically significant changes in Sab expression are indicated by (*) as calculated by a Student's t-test (p-value <0.005). BSA: Bovine serum albumin.

To more closely mimic the conditions that occur during adipogenesis, 3T3-L1 cells were grown to confluency and then 500 nM BSA-palmitate was added to the media for up to 7 days. The addition of 500 nM BSA-palmitate to the media increased Sab expression beginning at day 3, and this was sustained until day 6 before decreasing on day 7 (Fig. 11). This change in Sab

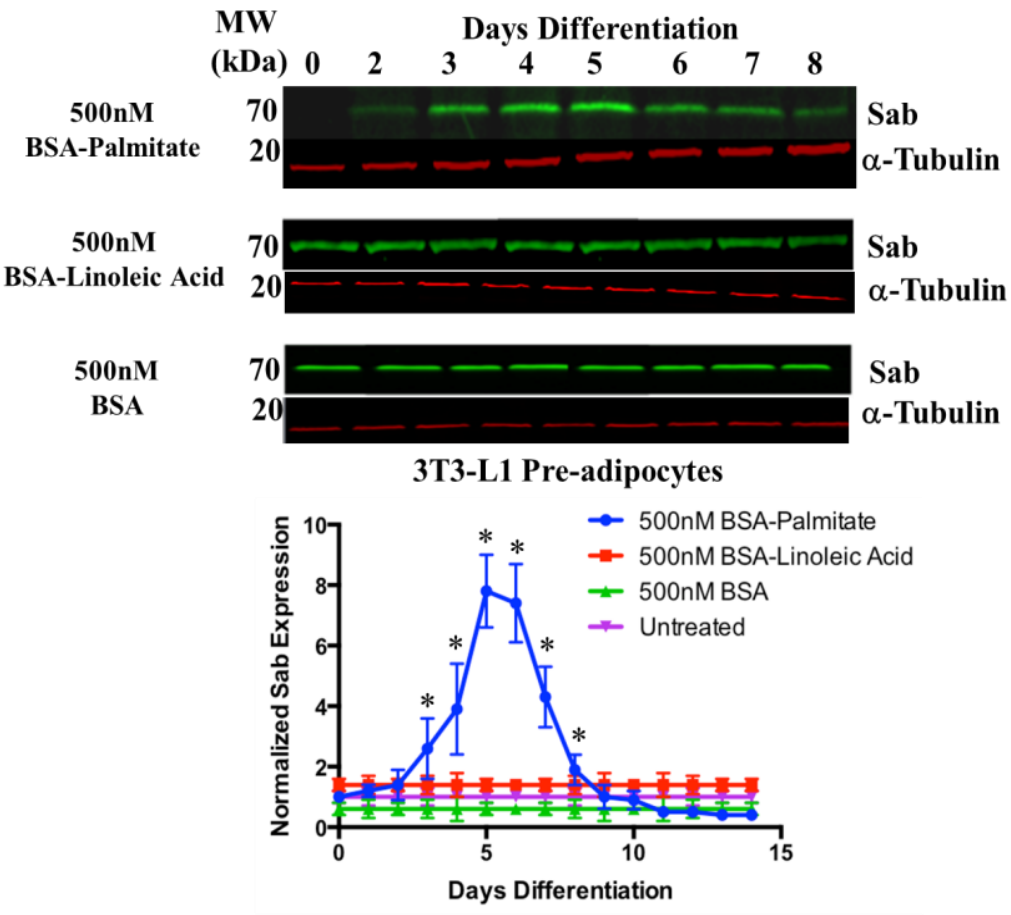

Figure 11: Chronic nutrient excess also increases Sab levels in 3T3-L1 pre-adipocytes. 3T3-L1 pre-adipocytes were grown to confluency and treated with 500 nM BSA-palmitate, BSA-linoleic acid, or BSA alone for up to 8 days. After treatment, cells were lysed and Sab levels were assessed by western blot analysis. Tubulin was used as a loading control. Sab levels were normalized to tubulin levels to determine the extent of Sab accumulation during the first half of adipogenesis. The values for BSA-Linoleic Acid and BSA Alone were off-set by 0.4 for viewing.Protein quantitation was performed using the ImageStudio® software package (bottom figure). Statistically significant changes in Sab expression are indicated by (*) as calculated by a Student's t-test and a Tukey's honest difference test to compare different treatments (p-value <0.005). BSA: Bovine serum albumin.

expression did not occur in cells treated with 500 nM BSA-linoleic acid (Fig. 11). Also, BSA alone (500 nM) did not induce a detectable change in Sab expression (Fig. 11). To confirm that nutrient excess occurred in 3T3-L1 cells during adipogenesis and in response to BSA-palmitate treatment, we analyzed the nutrient sensing pathways of the AMPK-dependent kinase and mTOR. During adipogenesis, when Sab levels were highest (day 3 to day 5), AMPKα is not phosphorylated (data not shown) and mTOR signaling is activated according to increased

Phospho-Raptor (an mTOR scaffold) levels (data not shown). This trend was observed in the presence of 500 nM BSA-palmitate (data not shown), but not in the presence of BSA-linoleic acid or BSA alone. These results demonstrate that Sab levels may change in response to metabolic changes, such as nutrient excess, during differentiation.

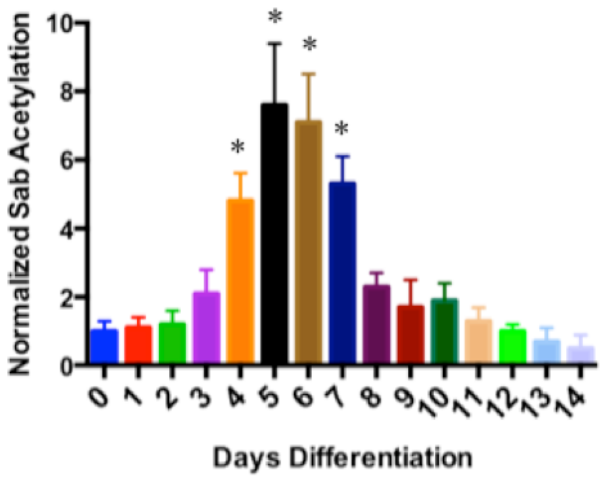

Figure 12: Sab is acetylated on lysine 6 during 3T3-L1 differentiation. To determine if Sab was acetylated during differentiation of 3T3-L1 pre-adipocytes into mature adipocytes, cells were subjected to the differentiation procedure and lysed on each day. The proteins for all days (0-14) were individually resolved by protein gel electrophoresis. Proteins bands between 60 and 75 kDa were excised from the gel and digested by trypsin. The peptides were then subjected to nano-electrospray injection tandem mass spectrometry. Mass to charge ratios were used to determine the presence of acetylated Sab (the peptide containing the acetylated K6 residue). Acetyl-Sab levels were normalized to the relative abundance of acetyl-Sab peptides in the day 0 sample, and then normalized to the N-terminal peptide of COX-IV to account for mitochondrial density. Statistically significant changes in Sab K6 acetylation are indicated by (*) as determined by the MSstat software (p-value <0.005).

3.5 Sab acetylation increases during adipogenesis

Preliminary studies in our lab had found that adipogenesis did not significantly impact the level of Sab mRNA in differentiating 3T3-L1 cells; therefore, it was proposed that post-translational modifications on Sab might stabilize the proteins during adipogenesis. Previous proteomic and bioinformatic analysis on Sab conducted in our lab revealed that Sab had two established phosphorylation sites at serines 351 and 421 and a novel acetylation site at lysine 6 (K6). Since the acetyl pool increases in differentiating adipocytes, we decided to monitor Sab acetylation on K6 during adipogenesis. To monitor Sab acetylation during adipogenesis, cells were lysed and resolved by protein gel electrophoresis. The proteins surrounding 70kDa were excised from the gel and digested by trypsin. Peptides were then identified using nano-electrospray injection tandem mass spectrometry. The N-terminal peptide of Sab was detected in both an unmodified and modified state in 3T3-L1 cells (data not shown). During adipogenesis, the frequency of the N-terminal peptide containing an acetylated K6 residue increased. The acetylated peptide began to increase on day 3 of adipogenesis until day 5, after day 5 the acetylated peptide decreased throughout the remainder of adipogenesis (Fig. 12). These data indicated that acetylation of Sab K6 parallels the increase in Sab levels on mitochondria. To confirm that the acetylation peptide was indeed K6 of Sab, we expressed a version of Sab expressing a C-terminal HaloTag for affinity purification (Fig 13A). We purified the

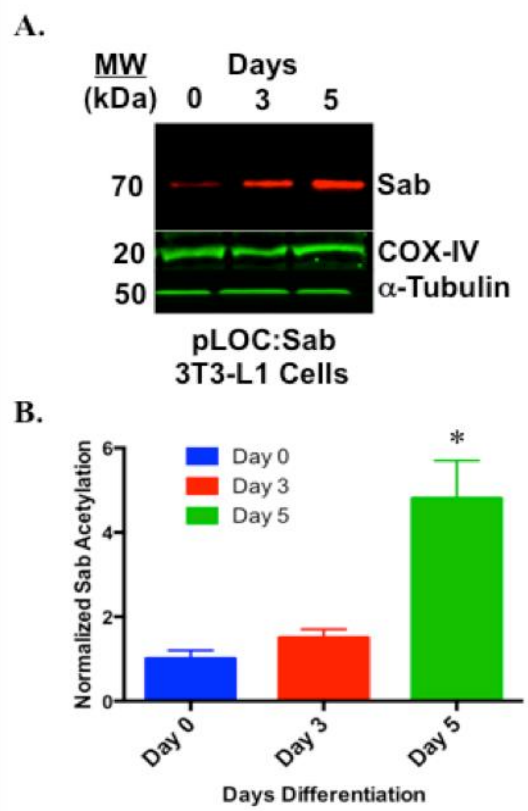

Figure 13: Purification of Sab during differentiation revealed increased acetylation on lysine 6. (A) The Sab ORF was cloned into a HaloTag expression to permit affinity purification using the HaloTag Ligand. The vector was then used to ectopically express the Sab:HaloTag in 3T3-L1 pre-adipocytes over 5 days. The cells were lysed on days 0, 3, and 5. The expression in the cells was examined for Sab, while tubulin and COX-IV were used as controls for loading and mitochondrial density, respectively. **(B)** 3T3-L1 cells were plated at a density of 2.5 x 10^5 cells per plate, and grown to confluency. Next, the cells were subjected to the first 5 days of the differentiation protocol. The cells were lysed. Sab was purified, and then analyzed for acetylation using nano-electrospray injection tandem mass spectrometry. Significant changes in Sab K6 acetylation are indicated by (*) as determined by the MSstat software (p-value <0.005). ORF: Open reading frame; COX-IV: Cytochrome c oxidase, or complex IV.

Sab:HaloTag from 3T3-L1 cells on days 0, 3, and 5 of adipogenesis. The purified Sab was prepared and analyzed by nano-electrospray injection tandem mass spectrometry for acetylation as described above. The level of Sab acetylated on K6 increased on days 3 and 5 (Fig. 13B). These data indicate that Sab is acetylated on K6 during adipogenesis.

3.6 Sab acetylation increases during nutrient excess

To determine if the increased acetylation of Sab was induced by the same physiological circumstances that elevated Sab levels in 3T3-L1 cells, we expressed the HaloTag-version of Sab for 72 hours, and then added 0.4 mM BSA-palmitate, BSA-linoleic acid, or BSA alone for 6 hours. The tagged version of Sab was then purified and submitted for mass spectrometry analysis. Compared to untreated 3T3-L1 cells, cells treated with 0.4 mM palmitate were found to have nearly a 8-fold increase in the acetylation of Sab K6 (Fig. 14A), and no acetylation change was observed in cells treated with 0.4 mM BSA-linoleic acid or BSA (Fig. 14A). To emulate the differentiation protocol, 3T3-L1 cells were grown in the presence of 500 nM BSA-palmitate, BSA-linoleic acid, or BSA alone for 5 days following confluency. Sab:HaloTag was expressed in these cells and purified following treatment. Mass spectrometric analysis of these cells demonstrated increased acetylation of Sab K6 on day 5 in cells treated with BSA-palmitate, while no change was observed for BSA-linoleic acid or BSA treated cells (Fig. 14B). These results indicate that the nutrient excess during adipogenesis may drive Sab acetylation.

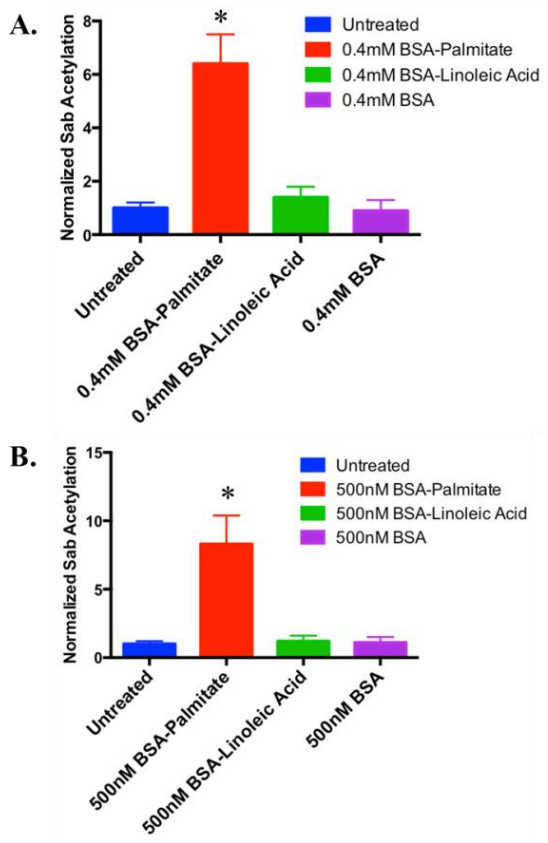

Figure 14: Acute and chronic nutrient excess promotes Sab acetylation on lysine 6. (A) 3T3-L1 cells were seeded at a density of 2.5 x 10^5 cells per 35-mm plate and transfected with a plasmid expressing a Sab-HaloTag fusion protein. Cells were grown to confluency (72 hours after transfection) and then treated with 0.4 mM BSA-palmitate, BSA-linoleic acid, or BSA alone for 6 hours. Cells were lysed and the Sab-HaloTag protein was purified and submitted to mass spectrometry based analysis of acetylation. **(B)** The same approach was employed for a sub-chronic treatment of 500 nM BSA-palmitate, BSA-linoleic acid, or BSA alone for 7 days. Acetylation of Sab was monitored using nano-electrospray injection tandem mass spectrometry. Statistically significant changes in Sab K6 acetylation are indicated by (*) as determined by the MSstat software (p-value <0.005). BSA: Bovine serum albumin.

3.7 Sab mislocalization after Sab:K6 mutation

To determine if the K6 acetylation site was critical to Sab function during adipogenesis, we generated two mutants of Sab; these were Sab:K6E, an acetylated mimicking mutant, and Sab:K6A, a null modified mutant. Mutagenesis was confirmed by sequencing of the respective plasmids. Next, the plasmids pLOC:Sab, pLOC:Sab:K6E, and pLOC:Sab:K6A were transfected into respective cultures of 3T3-L1 cells. Sab expression was monitored at 48 hours and 72 hours post-transfection by western blot analysis. According to western blots, all three proteins were expressed in 3T3-L1 cells (Fig. 15A) and mtTFA was used as a mitochondrial loading control (Fig. 15A). Mock transfected cells were treated with transfection reagent to provide a baseline for Sab expression in response to liposomal transfection (Fig. 15A). Cells were also transfected with pLOC:RFP (red fluorescent protein) to demonstrate that protein over-expression alone was not inducing Sab expression (Fig. 15A). However, immuno-fluorescence microscopy revealed that the Sab:K6E (Fig. 15Bii) and Sab:K6A (Fig. 15Biii) did not localize to mitochondria as compared to wild type Sab (Fig. 10Bi). Without the Sab variants localizing to the correct sub-cellular localization, we could not continue to evaluate the impact of mutating this residue in 3T3-L1 pre-adipocytes.

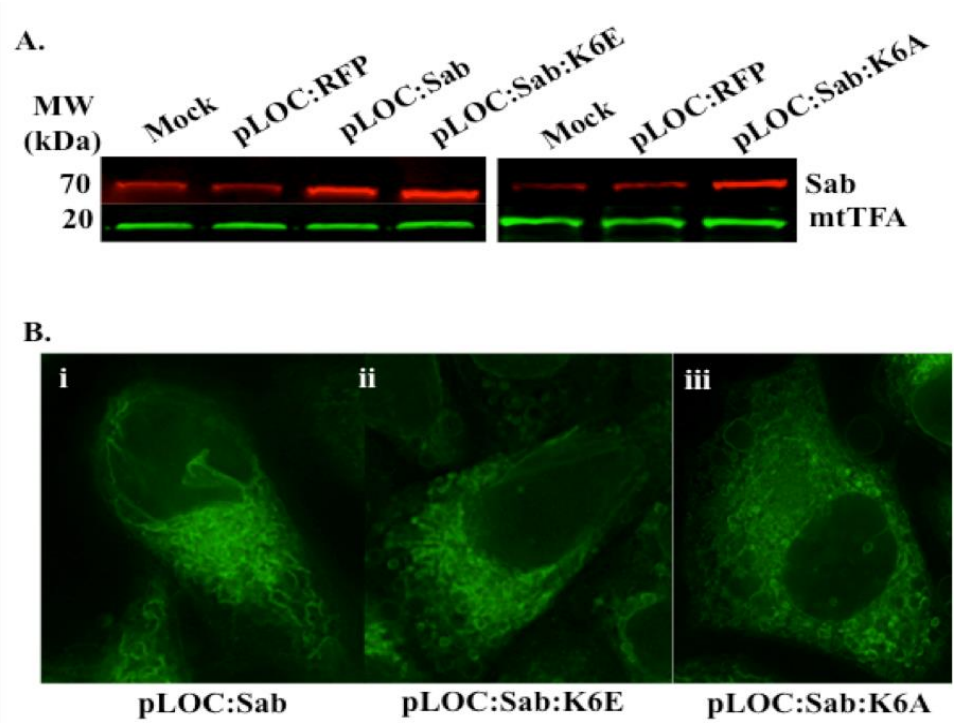

Figure 15: Ectopic expression of Sab variants Sab:K6E and Sab:K6A causes mislocalization of Sab. (A) Site-directed mutagenesis was employed to generate pLOC:Sab mutants K6E (a mutant mimicking acetylation on lysine 6) and K6A (an acetylation-null mutant). These plasmids were transfected into 3T3-L1 pre-adipocytes, and after 72 hours cells were lysed for western blot analysis of Sab levels. Tubulin was used as a cellular loading control, while COX-IV was used to determine the mitochondrial density of each sample. pLOC:RFP was included as a control to demonstrate that over-expression of a protein did not induce Sab expression. Mock cells were treated with transfection reagent to demonstrate that Sab was not induced by liposome-mediated transfection. **(B)** The 3T3-L1 pre-adipocytes were examined by immunofluorescent microscopy to assure proper localization of Sab to mitochondria (as observed in **(i)**). Neither the K6E variant **(ii)** nor K6A **(iii)** variant demonstrated typical mitochondrial localization. This aspect of research will require further investigation to determine if this is a valid approach. COX-IV: Cytochrome c oxidase, or complex IV; RFP: Red fluorescent protein.

3.8 Sab acetylation increases after inhibition of Sirtuin 3

Sirtuins are protein deacetylases that play a critical role in regulating cellular processes such as bioenergetics, mitochondrial biogenesis, and transcription. Therefore, we decided to silence sirtuins in 3T3-L1 cells and monitor the impact of specific sirtuin knockdowns on Sab acetylation. The relative expression of sirtuins 1-5 was silenced using siRNAs from Cell Based Screening Core at the Scripps Research Institute (Fig. 16A). Next, the respective siRNAs for each sirtuin were transfected into 3T3-L1 cells. The cells were lysed after 72 hours, and Sab was analyzed for acetylation using nano-electrospray injection tandem mass spectrometry. None of the sirtuins with the exception of SIRT3 had any impact on Sab acetylation (Fig. 16B). Silencing SIRT3 increased the amount of acetylated Sab in 3T3-L1 cells (Fig. 16B). This may suggest that SIRT3, a mitochondrial sirtuin, regulates Sab during adipogenesis to control mitochondrial density.

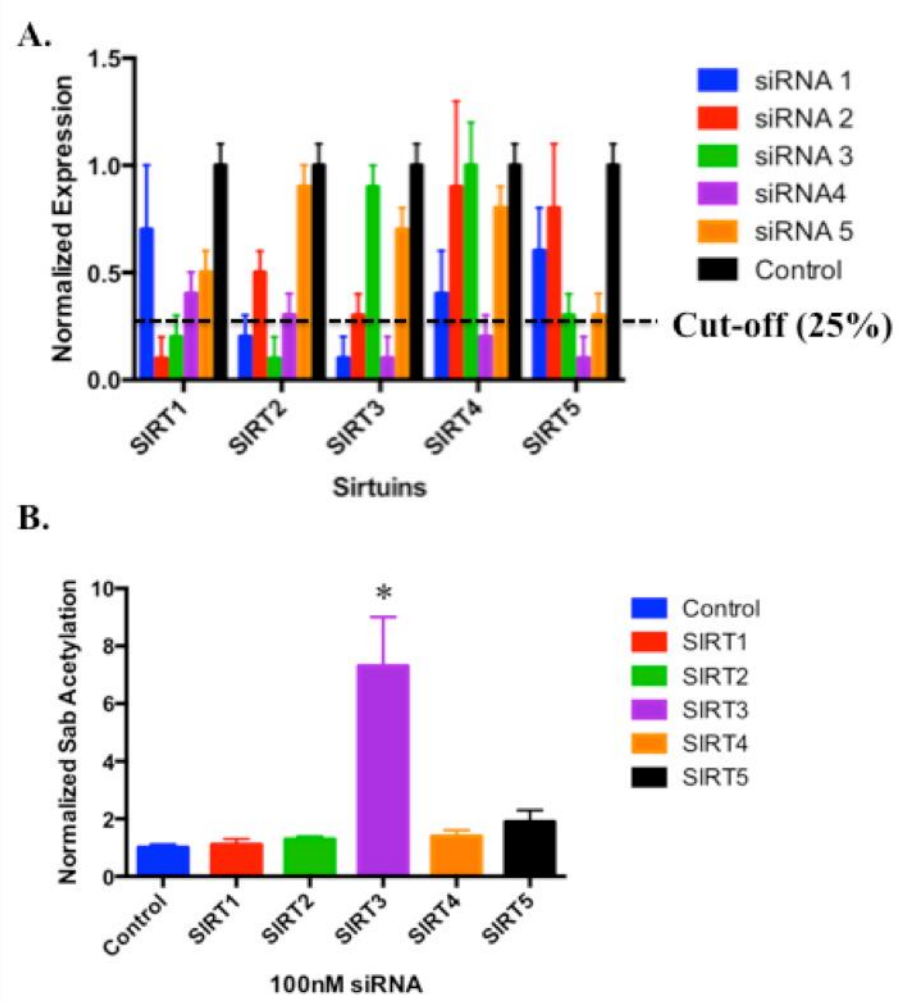

Figure 16: Silencing SIRT3 increases Sab acetylation in 3T3-L1 pre-adipocytes. (A) 3T3-L1 cells were plated at a density of 2.5 x 10^5 cells per 35-mm plate and transfected with siRNAs specific for each sirtuin. Five siRNAs were evaluated for each sirtuin. After 72 hours of silencing, cells were lysed and sirtuin levels were monitored by western blot analysis. The most effective siRNAs were used for additional studies. The cut-off value for ideal siRNAs was set at 75% knockdown (or 25% expression). Statistically significant changes in sirtuin expression were calculated by a Student's t-test and a Tukey's honest difference test to compare different treatments (p-value <0.005). **(B)** Cells were seeded into plates as described above, and then transfected with a plasmid encoding a HaloTag-version of Sab for protein purification. Following 24 hours, the cells were then transfected with siRNAs (100 nM) to silence the expression of individual sirtuins. Cells were lysed and Sab acetylation was determined by nano-electrospray injection tandem mass spectrometry. Significant changes in Sab K6 acetylation are indicated by (*) as determined by the MSstat software (p-value <0.005). siRNA: Small interfering ribonucleic acids.

Chapter 4
Discussion

4.1 Sab expression and signal transduction

Sab is one of the many proteins that interact with MAPK-pathways, which perform a wide variety of regulatory functions and cellular processes. Wiltshire *et al.* were the first to describe the interaction between Sab and JNK as a mechanism of mitochondrial localization (29). They also found that the kinase interaction motif 1(KIM1) of Sab is responsible for the JNK/Sab interaction. This was confirmed in our lab when we showed that inhibition of the JNK-KIM1 interaction disrupted translocation of JNK to the mitochondria and its localized functions (23).

JNK has previously been implicated in the reduction of mitochondrial content during the formation of adipocytes (10). In the present research project the role of Sab and the JNK/Sab interaction was investigated with regard to the initiation of mitophagy during adipogenesis. We were able to show that Sab levels and JNK activation (phosphorylation) increased between day 3 and 7 of adipocyte differentiation and that these events preceded the induction of autophagy genes (Fig. 6 and 7). Simultaneous exploration of adipogenesis genes like adiponectin, FABP4, and PPARγ revealed that these events occur in parallel with adipogenesis initiation (Fig. 6). Further, inhibition of the JNK/Sab interaction in our preliminary studies prevented reduction of mitochondrial density and adipogenesis. Taken together, these data suggest that Sab-mediated signaling may be responsible for the initiation of the mitophagy machinery, which is essential for adipogenesis. Other MAPKs may also attribute to the initiation of mitophagy and it is possible that phospho-p38 and phospho-ERK are part of the Sab-mediated signaling cascade that ultimately leads to mitophagy and adipogenesis initiation (Fig. 7).

The increase in Sab protein concentration during adipogenesis occurred after the addition of the differentiation agents insulin, dexamethasone, IBMX, and rosiglitazone. Treating the cells with these compounds individually did not increase Sab levels in the 3T3-L1 cells; further, the serum change from NCS to FBS did not impact Sab expression either (Fig. 8). Therefore, we concluded that the physiological culmination of these responses were responsible for the elevated Sab levels on mitochondria during adipogenesis. An early event in adipogenesis is the influx of both glycolytic and lipogenic substrates (30). When coupled with the production of fatty acids and lipids, the differentiating cells are in a state of nutrient

excess, which can lead to metabolic stress (13). Metabolic stress may thus increase Sab expression, which in turn interacts with JNK (or other MAPKs) and initiate the selective degradation of mitochondria. It has been show by previous research that JNK is capable of phosphorylating mitofusin 2 (Mfn2), a protein that prevents mitophagy (31). JNK mediated phosphorylation of Mfn2 leads to the ubiquitinylation and degradation of Mfn2 (31). This ultimately fragments the mitochondrial network setting the stage for mitophagy. Likewise, ERK1, another stress responsive MAPK, has been shown to phosphorylate and inhibit Mfn1 (32). ERK1 phosphorylation of Mfn1 also fragments the mitochondrial network (32). Sab may facilitate both events by sequestering JNK and ERK1 in close proximity to the mitofusins. This would explain why ectopic expression of Sab leads to fragmentation of the mitochondrial network and silencing Sab leads to a fused mitochondrial network (unpublished data from the Chambers lab). This work further establishes a physiological role for MAPKs in maintaining mitochondrial homeostasis.

Further research will be necessary to provide prove of true causality between the increase of Sab and the initiation of mitophagy and adipocyte differentiation.

4.2 Sab initiation and stabilization

While evidence suggests that acetylation of Sab might be necessary for stabilizing this scaffold protein, we were also interested in what stimulants caused it's increase and what started the cascade of mitochondrial degradation with respect to differentiation of adipocytes. Following the protocol of Zebisch *et al.*, there are several stress inducing agents that may cause the induction of Sab (28). As mentioned before, neither of these compounds could significantly increase Sab expression.

These results made us go back to our initial hypothesis of how an increased Sab stabilization is caused by acetylation of lysine 6. Acetylation is closely related with the metabolic status of the cell, and mitochondria are known to integrate these pathways. Furthermore, fatty acids can be a direct source for mitochondrial protein acetylation as shown with radio-actively labeled palmitate by Pougovkina *et al.* (34). Based on this knowledge we added palmitate as a source of FA to the differentiating 3T3-L1 pre-adipocytes.

Sab expression increased after 4 hours of treatment with 0.4 mM BSA-palmitate and no change was observed with the negative control or vehicle control (Fig. 10). The physiologically more relevant and sustained treatment with 500 nM BSA-palmitate increased Sab expression beginning at day 3, and continuing until day 6 (Fig. 11). These

results show both acute and chronic excess of nutrients are able to increase Sab expression. Obesity is also characterized by an excess of nutrients. This may lead to a state of metabolic confusion which increases Sab expression and starts the cascade of mitophagy initiation and adipogenesis. In obese patients this is related to an increased fat production.

4.3 Sab acetylation during adipogenesis

Mitochondria are the main organelles in which pyruvate, the end product of glycolysis, is converted into acetyl coenzyme A (acetyl Co-A), the necessary building block for the formation of fatty acids (10). Acetyl Co-A is also the major provider of acetyl groups for acetylation of proteins as a post-translational modification. During the formation of adipocytes there are two pathways extensively active: the glycolysis pathway due to excessive glucose and FA breakdown through β-oxidation (30). Both of these pathways increase the acetyl Co-A pool, and correlate with obesity since both glucose and FA levels are increased in these patients.

There is a difference in the handling of acetyl Co-A between brown adipose tissue (mitochondrial-rich) and white adipose tissue. Uncoupling protein 1 (UCP1) is extensively expressed in brown adipose, and also serves as a marker for this type of adipose tissue. This protein uncouples ATP synthesis from acetyl Co-A oxidation by dissipating the proton gradient (10). It can be considered that Sab inhibition, which would decrease the degradation of mitochondria, causes an increase in UCP1 expression and a shift in the handling of acetyl Co-A, which affects the acetylation status of mitochondrial proteins. This will be a topic of future research related to this project.

Changing the acetylation status of mitochondrial proteins can be considered as a way of metabolic regulation. Elevated levels of acetyl Co-A inside of the mitochondria affect cellular processes such as cell growth, proliferation, and metabolism (27). Mitochondria have a higher pH compared to the cytosol and a higher concentration of acetyl Co-A, which may form a preferable environment for non-enzymatic acetylation of proteins. Furthermore, several studies show that addition of acetyl Co-A, as well as high-fat diet increases the acetylation status of mitochondrial proteins (33). Thus, Sab may be acetylated by non-enzymatic or yet to be identified enzymatic processes within the mitochondrial intermembrane space.

For this project it was hypothesized that an increased pool of acetyl Co-A, would cause a higher amount of Sab acetylation, and hence stabilization on the OMM. We observed that

Sab increases before essential mitophagy proteins, and that this increase is associated with the time point of mitophagy initiation. Moreover, Sab was acetylated on lysine 6 during adipogenesis, specifically at the times where Sab was at its highest concentrations in differentiating 3T3-L1 cells (Fig. 12 and 13).

Since individual differentiation stimuli did not induce increased Sab levels in 3T3-L1 cells, we examined if the addition of palmitate increased Sab expression.

Acetyl-Sab was induced in high amounts after adding 0.4 mM palmitate for 6 hours, but this did not occur in linoleic acid or BSA treated cells (Fig. 14). These results show that acetylation of Sab is responsive to nutrient excess, possibly by means of a higher Sab stabilization on the OMM. This stabilization may be caused by higher concentrations of acetyl Co-A due to higher FA availability and oxidation. Actual measurements of acetyl Co-A during the course of adipogenesis fell out of the scope of this project, but would be an interesting future outcome.

Our results demonstrate that Sab acetylation coincides with metabolic changes associated with adipogenesis and metabolic stress. This may ultimately prove to be the mechanism that drives white adipose differentiation.

4.4 Sab regulation of mitochondrial density during adipogenesis

To further investigate the role of acetylation as a stabilizing factor in the regulation of mitophagy during adipogenesis, the most well-known deacetylating enzymes were inhibited and their impact was investigated using western blot analyses for the Sab protein. Our results show that SIRT3 inhibition significantly increased acetyl-Sab levels, while silencing other sirtuins had no impact on Sab acetylation under normal growth conditions (Fig. 16).

Interestingly, SIRT3 is known to be involved in metabolic regulation and adipogenesis. Caloric restriction induces SIRT3 expression; more specifically, caloric restriction equals less adipogenesis due to a decreased availability of nutrients, which is in agreement with our observations (35). It was also demonstrated that SIRT3 expression is decreased during adipogenesis and plays a critical role in fatty acid metabolism (36, 37). Finally, SIRT3 localizes to mitochondria, thus making it an ideal protein deacetylase for Sab (37). Taken together, it is clear that higher SIRT3 levels cause more protein deacetylation, which would destabilize the Sab expression on the OMM and prevent mitophagy as a critical factor to initiate adipogenesis. Therapeutic induction of SIRT3 may be a good target to prevent fat cells from being formed.

Previous research revealed a role of SIRT3 in the regulation of lysine acetylation of mitochondrial proteins (38). Our results show that when SIRT3 is inhibited, acetyl-Sab levels increase and this event correlates with the initiation of mitophagy. SIRT3 may be a control mechanism of the cell to keep mitophagy in check and coordinated. Existing research has demonstrated that SIRT3 is an essential component of mitochondrial biogenesis (39). Accordingly, deacetylation and destabilization of Sab on the OMM by SIRT3 may be a means to prevent mitochondrial turnover during adipogenesis. Thus, compounds capable of selectively enhancing SIRT3 activity may be useful anti-obesity agents.

4.5 The role of lysine 6 in Sab mitochondrial localization

Site-directed mutagenesis was performed to produce protein variants to simulate acetylated (K:E) and non-acetylated (K:A) states of Sab. Immuno-fluorescent microscopy of these protein variants revealed that neither localized to the mitochondria (Fig. 15). This is most likely attributed to the positive charge that is associated with lysine residues. These positive charges may be a necessity to localize to the mitochondria and allow Sab to perform is physiological function. Furthermore, these mutants formed insoluble aggregates in the cytosol, which may mean that Sab can only perform its role in close proximity of the mitochondria. Due to this fact, no further analyses for the specific role of lysine 6 in the control of Sab could be performed. However, studies using the recombinant versions of the mutants will be pursued in the future to evaluate protein stability, turnover, and interactions with OMM vesicles.

4.6 Closing Summary

Our results suggest that Sab and JNK signaling increase prior to the start of mitophagy. Previous data in our lab already showed that silencing Sab expression inhibited mito-JNK signaling but not nuclear JNK signaling. We were able to confirm with western blotting that this interaction is part of the early adipogenesis process, preceding the increase of autophagy proteins. Hence, Sab and JNK signaling may be responsible for the degradation of mitochondria. Further research is necessary to investigate the true nature of these proteins in coordination of mitophagy.

An increased acetyl Co-A pool as a result of increased glycolysis and FA oxidation, increases the cells acetylation capacity which is in favor of Sab stabilization an hence mitophagy. We demonstrated that this occurred by simulating nutrient excess with the addition of palmitate. Nutrient excess increased Sab expression and acetylation. Metabolic

stress associated with nutrient excess could then activate JNK (or other MAPKs) leading to mitochondrial dysfunction, fragmentation, and mitophagy in a Sab-dependent manner. The decreased mitochondrial density and higher availability of nutrients during obesity would favor the formation of fat cells. This is also confirmed by silencing SIRT3, a deacteylase that promotes mitochondrial biogenesis, which increases acetyl-Sab levels. Taken together, Sab-mediated signaling may regulate mitochondrial dynamics and cellular fate.

This research reveals several novel targets that can be further investigated as anti-obesity therapies. First of all specific targeting of Sab or the Sab/JNK interaction during adipogenesis could prevent the formation of more fat cells in response to nutrient excess in obesity. However Sab has been suggested to be involved in a wide variety of processes and diseases like non-alcoholic steatohepatitis, Alzheimer diseases, Parkinson disease and cancer (40-42). Therefore, it is unlikely that targeting this specific part of the pathway will show only effects during adipogenesis. Side-effects, such as inhibiting mitochondrial cell death responses, may limit the effectiveness of Sab as a therapeutic target. However, anti-obesity drugs seek to prevent fat accumulation, and by inhibiting Sab-mediated signaling in adipocytes, white adipose cells may be replaced by more energetic brown adipose cells leading to a leaner physique.

Targeting the acetylation of Sab is a better alternative to provide a more specific effect with fewer possibly dangerous consequences. Preventing Sab from being acetylated in response to an increased acetyl Co-A pool that arises from the increased nutrient availability might be an effective way to prevent or treat obesity. When mitophagy is not initiated, excessive white fat cells will not be formed, hence the detrimental effects of white adipose tissue are eliminated (15, 16). However, whole organism depletion of white adipose would result in further complications as well since white adipose is an endocrine organ and has roles in physiological homeostasis. As such, moderation should be employed when considering reducing white adipose tissue below healthy levels.

Further steps must be taken before an actual application of our research results can be achieved (*in vivo* models to prove causality, clinical trials with obese individuals, etc.). Nevertheless, application of the achieved knowledge will be beneficial for fundamental researchers, commercial companies that could exploit potential therapeutic or preventative outcomes and for patients who will ultimately benefit from these outcomes. Results obtained with this project are of great value for man and for society as it may eventually lead to a decrease in the prevalence of obesity and associated healthcare costs.

Chapter 5
Conclusion

During obesity, there is an energy imbalance in which nutrient intake exceeds energy expenditure. This nutrient excess increases the pool of acetyl Co-A used to fuel biosynthetic and bioenergetic processes. The enhanced availability also results in increased acetylation of metabolic proteins including mitochondrial proteins. Our work has demonstrated that the mitochondrial scaffold protein Sab facilitates adipogenesis. The topic of this research project was to determine what cellular contexts and events regulated Sab-mediated signaling during adipogenesis. We examined Sab expression levels during the differentiation of 3T3-L1 pre-adipocytes into mature adipocytes, and found that nutrient excess may lead to acetylation and subsequent stabilization of Sab. As a result of this increased acetyl-Sab, mitochondria were targeted for degradation. Since this is a critical event for the formation of fat cells, targeting Sab or the acetylation of Sab holds therapeutic potential for treatment of obesity.

The present study has some limitations. No true causality can be demonstrated between the acetylation of Sab and initiation of mitophagy. This would require an actual knock-out model, which could not be achieved in this project. There are probably multiple other factors involved in the initiation of mitophagy during adipogenesis and even if we can effectively target Sab or the Sab/JNK interaction, cells may find compensatory mechanisms to account for this loss and to still be able to perform mitophagy.

This project elucidated some of the basic molecular effects that are involved in mitophagy initiation, with regard to the involvement of Sab. Besides obesity, abnormal mitochondrial clearance is a hallmark of many different diseases. The knowledge acquired can potentially lead to new insides within many different fields.

Although this project did not intend to result in a direct clinical application, we were able to acquire some essential knowledge as to how mitophagy during adipogenesis is regulated and how it may be targeted in the future. This is a novel direction for the manipulation of adipocytes to cure or prevent obesity and to put an end to the ever growing epidemic of obesity. All together this research may be the beginning of a solution that ultimately leads to a decrease in the prevalence of obesity and the associated health care costs.

References

1. World Health Organization, Global status report on noncommunicable diseases 2014.
2. Obesity: preventing and managing the global epidemic. Report of a WHO consultation. World Health Organ Tech Rep Ser. 2000;894:i-xii, 1-253.
3. Guh DP, Zhang W, Bansback N, Amarsi Z, Birmingham CL, Anis AH. The incidence of co-morbidities related to obesity and overweight: a systematic review and meta-analysis. BMC Public Health. 2009;9:88.
4. Finkelstein EA, Trogdon JG, Cohen JW, Dietz W. Annual medical spending attributable to obesity: payer-and service-specific estimates. Health Aff (Millwood). 2009;28(5):w822-31.
5. Coelho M, Oliveira T, Fernandes R. Biochemistry of adipose tissue: an endocrine organ. Arch Med Sci. 2013;9(2):191-200.
6. Ali AT, Hochfeld WE, Myburgh R, Pepper MS. Adipocyte and adipogenesis. Eur J Cell Biol. 2013;92(6-7):229-36.
7. Rosen ED, Hsu CH, Wang X, Sakai S, Freeman MW, Gonzalez FJ, et al. C/EBPalpha induces adipogenesis through PPARgamma: a unified pathway. Genes Dev. 2002;16(1):22-6.
8. Gray SL, Dalla Nora E, Vidal-Puig AJ. Mouse models of PPAR-gamma deficiency: dissecting PPAR-gamma's role in metabolic homoeostasis. Biochem Soc Trans. 2005;33(Pt 5):1053-8.
9. De Pauw A, Tejerina S, Raes M, Keijer J, Arnould T. Mitochondrial (dys)function in adipocyte (de)differentiation and systemic metabolic alterations. Am J Pathol. 2009;175(3):927-39.
10. Zhang Y, Zeng X, Jin S. Autophagy in adipose tissue biology. Pharmacol Res. 2012;66(6):505-12.
11. Goldman SJ, Zhang Y, Jin S. Autophagic degradation of mitochondria in white adipose tissue differentiation. Antioxid Redox Signal. 2011;14(10):1971-8.
12. Kishi-Itakura C, Koyama-Honda I, Itakura E, Mizushima N. Ultrastructural analysis of autophagosome organization using mammalian autophagy-deficient cells. J Cell Sci. 2014;127(Pt 18):4089-102.
13. Liesa M, Shirihai OS. Mitochondrial dynamics in the regulation of nutrient utilization and energy expenditure. Cell Metab. 2013;17(4):491-506.
14. Tolkovsky AM. Mitophagy. Biochim Biophys Acta. 2009;1793(9):1508-15.
15. Baerga R, Zhang Y, Chen PH, Goldman S, Jin S. Targeted deletion of autophagy-related 5 (atg5) impairs adipogenesis in a cellular model and in mice. Autophagy. 2009;5(8):1118-30.
16. Zhang Y, Goldman S, Baerga R, Zhao Y, Komatsu M, Jin S. Adipose-specific deletion of autophagy-related gene 7 (atg7) in mice reveals a role in adipogenesis. Proceedings of the National Academy of Sciences of the United States of America. 2009;106(47):19860-5.
17. Singh R, Xiang Y, Wang Y, Baikati K, Cuervo AM, Luu YK, et al. Autophagy regulates adipose mass and differentiation in mice. The Journal of clinical investigation. 2009;119(11):3329-39.

18. Skop V, Cahova M, Dankova H, Papackova Z, Palenickova E, Svoboda P, et al. Autophagy inhibition in early but not in later stages prevents 3T3-L1 differentiation: Effect on mitochondrial remodeling. Differentiation. 2014.
19. Nguyen MT, Satoh H, Favelyukis S, Babendure JL, Imamura T, Sbodio JI, et al. JNK and tumor necrosis factor-alpha mediate free fatty acid-induced insulin resistance in 3T3-L1 adipocytes. J Biol Chem. 2005;280(42):35361-71.
20. Xu Z, Maroney AC, Dobrzanski P, Kukekov NV, Greene LA. The MLK family mediates c-Jun N-terminal kinase activation in neuronal apoptosis. Mol Cell Biol. 2001;21(14):4713-24.
21. Lei K, Davis RJ. JNK phosphorylation of Bim-related members of the Bcl2 family induces Bax-dependent apoptosis. Proc Natl Acad Sci U S A. 2003;100(5):2432-7.
22. Sabapathy K, Hochedlinger K, Nam SY, Bauer A, Karin M, Wagner EF. Distinct roles for JNK1 and JNK2 in regulating JNK activity and c-Jun-dependent cell proliferation. Mol Cell. 2004;15(5):713-25.
23. Chambers JW, Cherry L, Laughlin JD, Figuera-Losada M, Lograsso PV. Selective inhibition of mitochondrial JNK signaling achieved using peptide mimicry of the Sab kinase interacting motif-1 (KIM1). ACS chemical biology. 2011;6(8):808-18.
24. Chambers JW, LoGrasso PV. Mitochondrial c-Jun N-terminal kinase (JNK) signaling initiates physiological changes resulting in amplification of reactive oxygen species generation. The Journal of biological chemistry. 2011;286(18):16052-62.
25. Le Lay S, Simard G, Martinez MC, Andriantsitohaina R. Oxidative stress and metabolic pathologies: from an adipocentric point of view. Oxid Med Cell Longev. 2014;2014:908539.
26. Hirosumi J, Tuncman G, Chang L, Gorgun CZ, Uysal KT, Maeda K, et al. A central role for JNK in obesity and insulin resistance. Nature. 2002;420(6913):333-6.
27. Shi L, Tu BP. Protein acetylation as a means to regulate protein function in tune with metabolic state. Biochem Soc Trans. 2014;42(4):1037-42.
28. Zebisch K, Voigt V, Wabitsch M, Brandsch M. Protocol for effective differentiation of 3T3-L1 cells to adipocytes. Analytical biochemistry. 2012;425(1):88-90.
29. Wiltshire C, Matsushita M, Tsukada S, Gillespie DA, May GH. A new c-Jun N-terminal kinase (JNK)-interacting protein, Sab (SH3BP5), associates with mitochondria. Biochem J. 2002;367(Pt 3):577-85.
30. Rosen ED, Spiegelman BM. Molecular regulation of adipogenesis. Annual review of cell and developmental biology. 2000;16:145-71.
31. Leboucher GP, Tsai YC, Yang M, Shaw KC, Zhou M, Veenstra TD, et al. Stress-induced phosphorylation and proteasomal degradation of mitofusin 2 facilitates mitochondrial fragmentation and apoptosis. Mol Cell. 2012;47(4):547-57.
32. Pyakurel A, Savoia C, Hess D, Scorrano L. Extracellular regulated kinase phosphorylates mitofusin 1 to control mitochondrial morphology and apoptosis. Mol Cell. 2015;58(2):244-54.

33. Weinert BT, Iesmantavicius V, Moustafa T, Schölz C, Wagner SA, Magnes C, et al. Acetylation dynamics and stoichiometry in Saccharomyces cerevisiae. Mol Syst Biol. 2014;10:716.
34. Pougovkina O, te Brinke H, Ofman R, van Cruchten AG, Kulik W, Wanders RJ, et al. Mitochondrial protein acetylation is driven by acetyl-CoA from fatty acid oxidation. Hum Mol Genet. 2014;23(13):3513-22.
35. Shi T, Wang F, Stieren E, Tong Q. SIRT3, a mitochondrial sirtuin deacetylase, regulates mitochondrial function and thermogenesis in brown adipocytes. J Biol Chem. 2005;280(14):13560-7.
36. Hirschey MD, Shimazu T, Goetzman E, Jing E, Schwer B, Lombard DB, et al. SIRT3 regulates mitochondrial fatty-acid oxidation by reversible enzyme deacetylation. Nature. 2010;464(7285):121-5.
37. Yu J, Auwerx J. The role of sirtuins in the control of metabolic homeostasis. Ann N Y Acad Sci. 2009;1173 Suppl 1:E10-9.
38. Lombard DB, Alt FW, Cheng HL, Bunkenborg J, Streeper RS, Mostoslavsky R, et al. Mammalian Sir2 homolog SIRT3 regulates global mitochondrial lysine acetylation. Mol Cell Biol. 2007;27(24):8807-14.
39. Giralt A, Villarroya F. SIRT3, a pivotal actor in mitochondrial functions: metabolism, cell death and aging. The Biochemical journal. 2012;444(1):1-10.
40. Win S, Than TA, Le BH, García-Ruiz C, Fernandez-Checa JC, Kaplowitz N. Sab (Sh3bp5) dependence of JNK mediated inhibition of mitochondrial respiration in palmitic acid induced hepatocyte lipotoxicity. J Hepatol. 2015;62(6):1367-74.
41. Takeshita Y, Hashimoto Y, Nawa M, Uchino H, Matsuoka M. SH3-binding protein 5 mediates the neuroprotective effect of the secreted bioactive peptide humanin by inhibiting c-Jun NH2-terminal kinase. J Biol Chem. 2013;288(34):24691-704.
42. Chambers JW, Howard S, LoGrasso PV. Blocking c-Jun N-terminal kinase (JNK) translocation to the mitochondria prevents 6-hydroxydopamine-induced toxicity in vitro and in vivo. The Journal of biological chemistry. 2013;288(2):1079-87.

Auteursrechtelijke overeenkomst

Ik/wij verlenen het wereldwijde auteursrecht voor de ingediende eindverhandeling:
Regulation of mitophagy by Sab during adipogenesis

Richting: **master in de biomedische wetenschappen-klinische moleculaire wetenschappen**
Jaar: **2015**

in alle mogelijke mediaformaten, - bestaande en in de toekomst te ontwikkelen - , aan de Universiteit Hasselt.

Niet tegenstaand deze toekenning van het auteursrecht aan de Universiteit Hasselt behoud ik als auteur het recht om de eindverhandeling, - in zijn geheel of gedeeltelijk -, vrij te reproduceren, (her)publiceren of distribueren zonder de toelating te moeten verkrijgen van de Universiteit Hasselt.

Ik bevestig dat de eindverhandeling mijn origineel werk is, en dat ik het recht heb om de rechten te verlenen die in deze overeenkomst worden beschreven. Ik verklaar tevens dat de eindverhandeling, naar mijn weten, het auteursrecht van anderen niet overtreedt.

Ik verklaar tevens dat ik voor het materiaal in de eindverhandeling dat beschermd wordt door het auteursrecht, de nodige toelatingen heb verkregen zodat ik deze ook aan de Universiteit Hasselt kan overdragen en dat dit duidelijk in de tekst en inhoud van de eindverhandeling werd genotificeerd.

Universiteit Hasselt zal mij als auteur(s) van de eindverhandeling identificeren en zal geen wijzigingen aanbrengen aan de eindverhandeling, uitgezonderd deze toegelaten door deze overeenkomst.

Voor akkoord,

Goubert, Désirée

Datum: **11/06/2015**